Materials Today Bio 25 (2024) 100950

Contents lists available at ScienceDirect

Materials Today Bio

journal homepage: www.journals.elsevier.com/materials-today-bio

Revealing an important role of piezoelectric polymers in nervous-tissue regeneration: A review

Lada E. Shlapakova [a,**], Maria A. Surmeneva [a,b,***], Andrei L. Kholkin [b,c,*], Roman A. Surmenev [a,b,****]

[a] Physical Materials Science and Composite Materials Center, Research School of Chemistry & Applied Biomedical Sciences, National Research Tomsk Polytechnic University, Tomsk, 634050, Russia
[b] Piezo- and Magnetoelectric Materials Research & Development Centre, Research School of Chemistry & Applied Biomedical Sciences, National Research Tomsk Polytechnic University, 634050, Tomsk, Russia
[c] Department of Physics & CICECO - Aveiro Institute of Materials, University of Aveiro, 3810-193, Aveiro, Portugal

ARTICLE INFO

Keywords:
Piezoelectric polymer
Polyvinylidene fluoride
poly(L-lactic acid)
Polyhydroxyalkanoate
Nerve guidance conduit

ABSTRACT

Nerve injuries pose a drastic threat to nerve mobility and sensitivity and lead to permanent dysfunction due to low regenerative capacity of mature neurons. The electrical stimuli that can be provided by electroactive materials are some of the most effective tools for the formation of soft tissues, including nerves. Electric output can provide a distinctly favorable bioelectrical microenvironment, which is especially relevant for the nervous system. Piezoelectric biomaterials have attracted attention in the field of neural tissue engineering owing to their biocompatibility and ability to generate piezoelectric surface charges. In this review, an outlook of the most recent achievements in the field of piezoelectric biomaterials is described with an emphasis on piezoelectric polymers for neural tissue engineering. First, general recommendations for the design of an optimal nerve scaffold are discussed. Then, specific mechanisms determining nerve regeneration via piezoelectric stimulation are considered. Activation of piezoelectric responses via natural body movements, ultrasound, and magnetic fillers is also examined. The use of magnetoelectric materials in combination with alternating magnetic fields is thought to be the most promising due to controllable reproducible cyclic deformations and deep tissue permeation by magnetic fields without tissue heating. *In vitro* and *in vivo* applications of nerve guidance scaffolds and conduits made of various piezopolymers are reviewed too. Finally, challenges and prospective research directions regarding piezoelectric biomaterials promoting nerve regeneration are discussed. Thus, the most relevant scientific findings and strategies in neural tissue engineering are described here, and this review may serve as a guideline both for researchers and clinicians.

1. Introduction

The nervous system controls every organ and system in an organism and consists of two parts: the central nervous system (CNS) and peripheral nervous system (PNS). Signaling pathways go from the CNS to other parts of the body via the PNS. Unlike the CNS, owing to the lack of shielding by bone tissue and the blood–brain barrier, the PNS is more susceptible to injuries, e.g., due to disease, toxins, surgical procedures, accidents, or natural disasters. As a result, peripheral nerve injuries (PNIs) may pose a threat to nerve mobility and sensitivity and possibly lead to permanent function loss due to the low regenerative capacity of mature neurons [1–4]. More than 300,000 PNI cases in Europe and 20,

* Corresponding author. Piezo- and Magnetoelectric Materials Research & Development Centre, Research School of Chemistry & Applied Biomedical Sciences, National Research Tomsk Polytechnic University, 634050, Tomsk, Russia.
** Corresponding author.
*** Corresponding author. Physical Materials Science and Composite Materials Center, Research School of Chemistry & Applied Biomedical Sciences, National Research Tomsk Polytechnic University, Tomsk, 634050, Russia.
**** Corresponding author. Physical Materials Science and Composite Materials Center, Research School of Chemistry & Applied Biomedical Sciences, National Research Tomsk Polytechnic University, Tomsk, 634050, Russia.
E-mail addresses: les2@tpu.ru (L.E. Shlapakova), surmenevamaria@mail.ru (M.A. Surmeneva), kholkin@ua.pt (A.L. Kholkin), rsurmenev@mail.ru (R.A. Surmenev).

https://doi.org/10.1016/j.mtbio.2024.100950
Received 5 October 2023; Received in revised form 12 December 2023; Accepted 8 January 2024
Available online 11 January 2024

000,000 cases in the United States are reported annually [1,4]. Severe nervous-system injuries currently have limited therapeutic options. Small PNI sites are capable of spontaneous self-regeneration, wherein Schwann cells (SCs) reorganize and migrate to form bands of Büngner, which act as longitudinal guides for the regrowth of axons from the proximal to the distal nerve stump [5]. In more extended gaps, nerve regeneration is a sensitive and slow process, where a guiding pathway is essential for protection and stimulation at the same time.

Currently, the most widely clinically used approach to PNI treatment is autologous grafting, wherein a donor nerve is resected and transplanted into an injury site of the same person. Autografts supply the regenerating axons with a natural guidance channel populated with functioning SCs. Although this method is considered the gold standard, it is still far from ideal, for example, due to donor site morbidity, donor shortage, a mismatch between the donor and damaged nerves, and risks of infections or neuroma formation, resulting in a second surgical operation [2,3,6–8]. Therefore, biomaterials appear to be more advantageous for nerve tissue repair because of their structural and chemical versatility and accessibility. Polymers possess attractive properties for biomedical applications. They are light-weight, inexpensive, and easily processable; they show excellent compatibility with other organic and inorganic materials for the development of multifunctional hybrid systems; and some polymers are biodegradable and biocompatible [9,10]. In the context of neural tissue engineering, polymers can be processed into nerve guidance conduits (NGCs), which are tubular constructs into which proximal and distal stumps of an injured nerve can be inserted [4,6,11–15]. The axons regenerating from the proximal stump grow through the conduit toward the distal stump. Trophic support for both stumps is provided by the conduit, which also prevents invasion of the gap (between the stumps) by surrounding tissues. In addition to their use in repair of peripheral-nerve lesions, conduits can be utilized to wrap a repair site after end-to-end reconstruction of nerves in order to reduce scarring and for the treatment of neuromas [16].

Biocompatible and biodegradable conduits have been introduced that resorb in physiological environments with no adverse effects; however, they have acted only as tubes bridging the distal and proximal stumps and failed to provide necessary stimulatory cues for nerve regeneration [2]. Accordingly, the greatest promise is shown by the supplying of such nerve guides with appropriate stimuli to provoke nerve lesion repair; in this regard, electrical stimulation is more efficient for soft tissues such as skin, cardiac, and nervous tissues [2,6,17–19]. Electrical stimuli can guide regenerating axons across the nerve gap to connect with the distal stump of the injured nerve via biological signal transduction. SCs stimulated by an electric field of 50 mV/mm show increased neurite outgrowth and greater alignment in the direction of the applied electric field [20]. On this evidence, electroconductive conduits have been investigated [21–24] that can support an electrical environment of artificially generated electric fields necessary for efficient nerve regeneration. For example, Phamornnak et al. [25] have developed electroactive microfibrous scaffolds based on silk fibroin (SF) and poly (3,4-ethylenedioxythiophene):polystyrene sulfonate (PEDOT:PSS) for peripheral neural tissue engineering. The latest developments in the field of conductive NGCs have been systematically summarized in a review paper [2]. Electrical stimulation by means of such conduits generally requires auxiliary devices, such as electrodes, to generate electric fields. Nonetheless, the need for a complex circuit system with an external power source, inflammation caused by implanted electrodes, and the necessity of a second surgery to remove the electrodes limit clinical applications of this approach [20,26–28]. Contrary to the conventional electrical stimulation, wireless and self-powered devices based on piezoelectric polymers can deliver electrical stimuli without external energy sources or electrodes [29–32]. A piezoelectric polymer can develop a voltage when a mechanical stress is applied or vice versa [33–36]. Polyvinylidene difluoride (PVDF), poly (L-lactic acid) [PLLA], poly (3-hydroxybutyrate) [PHB], and many of their copolymers are widely used for neural tissue engineering applications. Piezoelectric polymeric conduits have been shown to facilitate SC adhesion, proliferation, and expression of functional proteins *in vitro* as well as to accelerate nerve conducting velocity, promote axonal remyelination, and restore motor function *in vivo* [37]. Furthermore, a piezoelectric boron nitride–functionalized polymer conduit can induce microvessel regrowth into neurons and reverses muscular atrophy after denervation in a model of a severe sciatic nerve defect [38].

Piezoelectricity in various biological tissues and recent advances in the fabrication and application of piezoelectric scaffolds have been summarized in some reviews [39,40]. A review by Zaszczynska et al. [41] describes the piezoelectric materials most frequently used for neural tissue engineering together with the main achievements, challenges, and future needs for research and treatments. In 2022, Askari et al. [42] presented a review on piezoelectric composites in neural tissue engineering; that paper deals with hybrid materials based on piezoceramics and piezopolymers as well as methods of their fabrication. In that paper, only PVDF and its copolymer-based scaffolds are considered, while other piezopolymers, such as PLLA and PHB, are not mentioned. A very recent review by Xu et al. [43] classifies piezoelectric materials and examines methods providing piezoelectric stimuli, including ultrasonication and mechanical movements of the human body, such as muscle contraction and relaxation and blood flow, as well as micromovements involved in cell migration, which can cause deformation of piezoelectric materials to induce electrical output.

The analysis of the literature allowed to reveal that at the moment, on the subject of piezopolymeric materials for neural tissue engineering, there are no systematic detailed reviews that not only contain the latest developments in piezoelectric nerve guidance devices but also integrate these efforts of many years into general recommendations for the design of efficient NGCs for specific nerve injuries. Moreover, the published reviews do not explain possible mechanisms of piezoelectric stimulation of neuronal cells and tissues. Therefore, the aim of this review was to compile *in vitro* and *in vivo* studies of nerve scaffolds and conduits based on commonly used piezoelectric polymers and composites. First, general recommendations for the design of efficient NGCs are provided with special attention to electrospun NGCs. Then, the mechanisms underlying electrical stimulation of neural tissue regeneration are thoroughly considered. Next, published findings about nerve scaffolds based on PVDF, PLLA, PHB, and their composites are discussed, as are their main advantages, biological outcomes, and future challenges.

2. Requirements for the design of piezoelectric nerve scaffolds

2.1. Biocompatibility and biodegradability

A number of requirements should be considered when NGCs with maximized efficiency are designed. Primarily, a nerve scaffold must be biocompatible, i.e., not evoke any mutagenic, carcinogenic, and cytotoxic effects or inflammatory responses. Generally, synthetic piezoelectric polymers have the advantage of biocompatibility, which can be additionally enhanced via the introduction of natural polymers. For instance, incorporation of type I collagen among PHB/PHBV nanofibers increases SC proliferation, *GDNF* mRNA expression, and NGF secretion, meaning stimulated cell differentiation [44].

Furthermore, an NGC must be biodegradable, so that it is resorbed in the human body at a rate consistent with that of the nerve restoration. After the implant is sutured at the nerve stumps, the biodegradable scaffold can be populated and remodeled by neuronal cells and eventually replaced by the native tissue; hence, the original function can be restored without a second surgery. The biodegradation rate is a critical parameter of an NGC because it must provide sufficient support for nerve tissue throughout the whole regeneration period. The resorption rate of biodegradable piezoelectric polymers can be adjusted via blending with other polymers. For example, the addition of up to 20 wt% of chitosan to PHB nerve scaffolds increases their mass loss from 20 % to 35 % after 8 weeks of degradation in PBS [45]. Polymers mounting the

Table 1
Mechanical properties of nerve tissues.

Nerve	Ultimate tensile strength, MPa	Elongation at break, %	Young's modulus, MPa	Ref.
Rat sciatic nerve	6.1 ± 1.5	49.2 ± 2.4	13.79 ± 5.48	[58]
Rat spinal nerve dendrites	0.62 ± 0.31	30.8 ± 8.4	2.9 ± 1.5	[59]
Human sciatic nerve	–	–	40.96 ± 2.59	[60]
Human peroneal middle nerve	3.88 ± 1.47	~60 %	10.41 ± 2.85	[61]
Human tibial middle nerve	3.91 ± 0.92	~35 %	9.50 ± 2.84	
Rabbit tibial nerve	11.7 ± 7.0	38.5 ± 2.0	–	[62]

strongest piezoelectric response, i.e., PVDF and its copolymers, are nondegradable. This issue has been addressed by blending PVDF with degradable nonpiezoelectric materials [11,12,31], resulting in worsened piezoelectric properties. In one study [31], nondegradable PVDF was blended with PCL to fabricate an electroactive NGC, which lost up to 9.1 % of mass during a 4-month period *in vivo*, and this loss was appropriate for long-term mechanical support for nerve regrowth within the conduit. To maintain desired piezoelectric signals, PVDF and its copolymers should be blended with degradable piezoelectric polymers, i.e., PLLA or PHB.

2.2. Piezoelectric capacity

Biocompatible and biodegradable conduits have been introduced that degrade in physiological environments with no adverse effects but act only as tubes bridging the distal and proximal stumps and have failed to provide necessary stimulatory cues for nerve regeneration [2]. Besides biocompatibility and biodegradability, NGCs obviously need to be bioactive. Promising effects of electrical stimulation on neural cell proliferation and differentiation *in vitro* and tissue growth *in vivo* have aroused interest in the use of piezoelectric scaffolds for neural tissue repair. For instance, piezoelectric P(VDF-TrFE) electrospun scaffolds with aligned fibers have been shown to promote adhesion, proliferation, myelination, and neurite extension of SCs [46–48]. In turn, when applied to a 10-mm rat sciatic nerve defect for 12 weeks, a self-powered electroconductive NGC with aligned electrospun PLLA fibers significantly facilitated peripheral nerve regeneration and enhanced motor functional recovery as evidenced by an improved sciatic function index (SFI), compound muscle action potential (CMAP), and muscle weights [29].

2.3. Sufficient strength and flexibility

Porosity and permeability are important for robust nerve regeneration, while the biodegradability of NGCs allows to avoid a second surgical operation. At the same time, NGCs must retain sufficient mechanical strength and integrity for long-term physical support and protection of the regenerating nerves. Mechanical roles of NGCs are as follows: to create a barrier protecting new axons from the forming scar tissue, to prevent compression of the regenerating cells by the surrounding tissue, and to provide stable structural support until there is sufficient regeneration of the nerve [3]. Given that peripheral nerves are subject to stretching, compression, and shearing forces, an NGC must also be flexible to withstand these forces and allow for the bending of joints without nerve compression [3,7]. In addition, an NGC has to resist the tearing, breaking, or cracking resulting from manipulations and sutures. To construct NGCs of appropriate strength and flexibility, mechanical properties of a target area have to be estimated. As demonstrated in Table 1, nerve tissues are very flexible and ductile, with high values of elongation at break (30 %–60 %) and low Young's moduli. Stiffness has been reported to direct differentiation of nonhuman neural stem cells (NSCs), with neuronal differentiation preferred on softer hydrogel matrices [49]. Most of piezoelectric polymers generally are unsuitably strong or stiff to mimic a nervous tissue [7]. Such polymers as PHAs, PLLA, and PVDF have Young's moduli that are often orders of magnitude greater than that of a native nerve [7]. Therefore, these polymers are often blended with more ductile polymers to reduce their inherent stiffness. For example, PHB, which is intrinsically brittle and has too high Young's modulus and insufficient elongation at break to meet the requirements of NGCs [44,50], is often blended with PCL, chitosan, or other PHAs [5,45,51,52], or copolymers are used instead, such as P (3HB-co-4HB) [5], PHBHHx [53,54], or poly (3-hydroxybutyrate-*co*-3-hydroxyvalerate) [PHBV] [44,55–57]. Among polyesters, only PCL-based polymers possess the mechanical properties that even approach those of a native nerve tissue [7]. The addition of PCL has been shown to improve the bending and tensile properties of PHB [5]. Furthermore, a blend of PCL with PVDF simultaneously improves mechanical properties, biocompatibility, and biodegradation of PVDF while retaining desired piezoelectricity [31]. Finally, blending with a natural piezoelectric biopolymer collagen can also address the issue of stiffness of synthetic piezoelectric polyesters [55].

2.4. Optimal fabrication method

Numerous techniques for fabrication of piezoelectric NGCs exist, such as salt leaching, freeze-drying, dip-coating, self-assembly, solvent casting, gas foaming, 3D printing, and electrospinning [6]. The majority of these techniques have drawbacks limiting their applications to NGC manufacturing. For example, self-assembly does not offer precise control over fiber dimensions; poor interconnectivity of pores, small pore size, and irregular porosity are the main drawbacks of gas foaming and freeze drying [3]. Low mechanical strength limits the range of applications of 3D-printed scaffolds [63].

Recently, the feasibility of additive manufacturing for the construction of conduits with 3D continuous conductive network structure was demonstrated in Ref. [64]. An efficient NGC was constructed by prior powder design and laser additive manufacturing. In particular, the PLLA particle surface was coated with $Ti_3C_2T_x$ (MXene) by ultrasound-assisted solution mixing and thus MXene was enriched at interfacial regions among adjacent polymer particles to form a continuous MXene conductive network. Cell assays confirmed that the conduits significantly promote cell proliferation, differentiation, and neurite outgrowth [64].

Electrospinning allows for the formation of 3D structures that successfully mimic the native extracellular matrix (ECM). The porosity, flexibility, and large surface area of electrospun fibrous mats can create an enhanced environment for cell–substrate interactions. Generally, to induce β-phase formation in crystalline structure of piezoelectric PVDF, poling with heat treatment is employed [31,33,49,65–69]. Nonetheless, electrospun PVDF scaffolds can manifest piezoelectricity without the post-poling process because poling is carried out during electrospinning, owing to the applied electric forces and polymer jet elongation [33,66,70–72]. The strain induced in the electrospinning solution causes uniaxial elongation of PVDF molecular chains along the fiber axis, thereby leading to β-phase formation. Additionally, the β-phase content can be controlled by varying parameters of electrospinning (voltage, needle tip–collector distance, and the flow rate), the solution (PVDF molecular weight and solvent), or the environment (humidity and temperature) [71].

Moreover, it has been found that the crystallinity of an electrospun polymer directly correlates with the fiber diameter [73,74]. The latter can be adjusted by varying the parameters of electrospinning [63]; accordingly, crystallinity and consequently piezoelectricity also strongly depend on the electrospinning process. Tai et al. [30] have obtained electrospun PLLA scaffolds with aligned fibers of 30–500 nm and found fiber diameter- and heat treatment–dependent changes in phase contents, which affected piezoelectric performance in transverse and

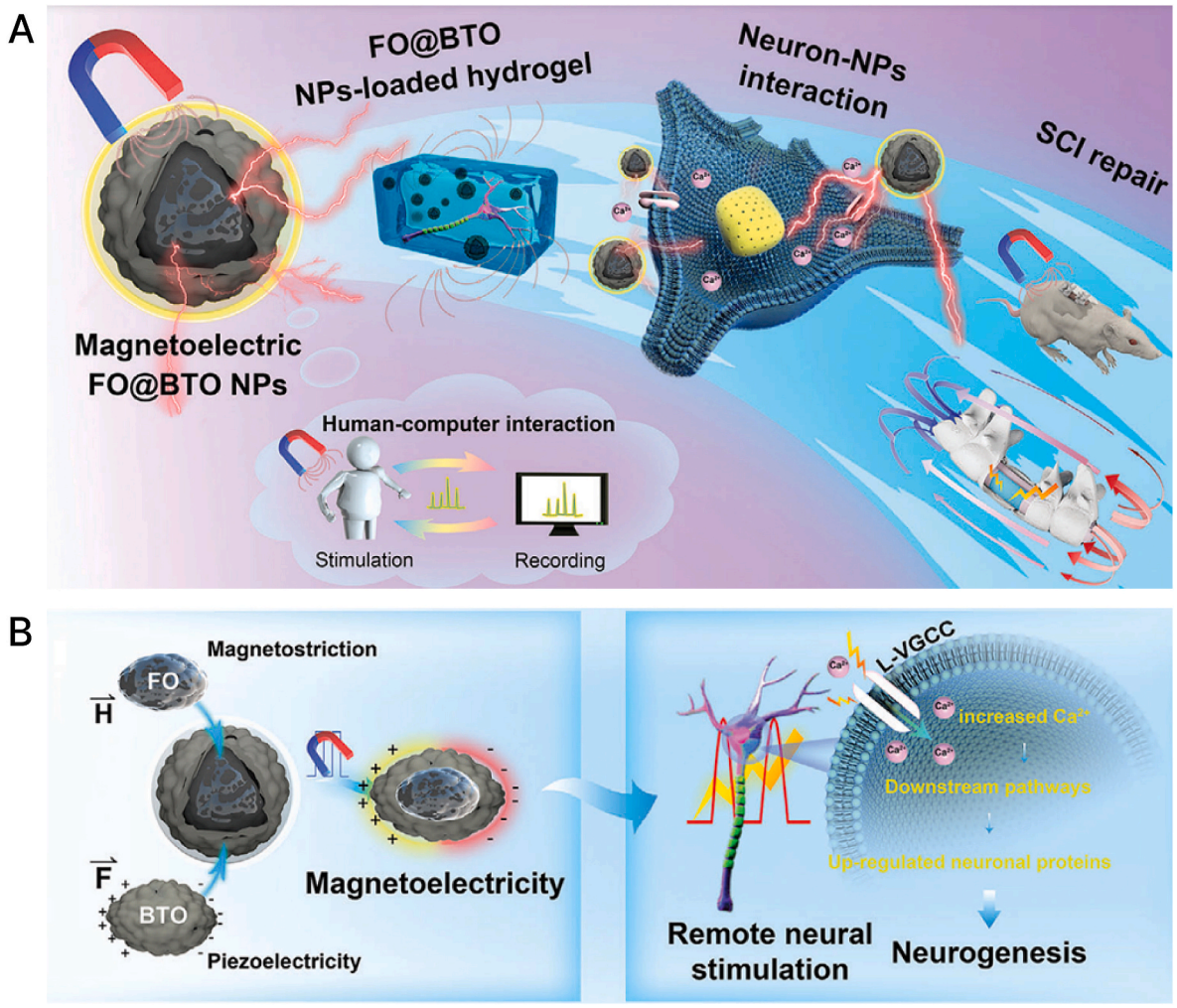

Fig. 1. Magnetoelectric nanoparticles for electrostimulation of nerve injury repair. (A) Schematic illustration of remote electrical stimulation induced by magnetoelectric Fe_3O_4@$BaTiO_3$ nanoparticles (FO@BTO). (B) A diagram of the interaction between magnetoelectric nanoparticles and neural cells. NPs: nanoparticles, SCI: spinal cord injury, VGCC: voltage-gated calcium channel. Reprinted from Ref. [92] with permission from Wiley.

longitudinal directions. Thus, electrospinning is a versatile, simple, low-cost, and controllable technique, which can produce defect-free NGCs with precisely tailored fiber architecture, crystallinity, and piezoelectricity. Fibers' properties can be tuned by adjustment of electrospinning-solution and process parameters and environmental conditions [1,63].

2.5. Improving surface water wettability of piezoelectric polymers

Water wettability of a polymer surface (i.e., hydrophobicity vs. hydrophilicity) is known to be one of the key factors influencing cell–material interaction and subsequent cell behaviors. Wettability of a surface can be strongly affected by surface functional groups [57,75–78] and surface roughness of the material [50,79–86]. Normally, cells prefer a surface of moderate hydrophilicity for adhesion and growth, whereas polymer surfaces featuring superhydrophilicity (contact angle below 5°) or superhydrophobicity (contact angle above 150°) are not favorable for cell attachment and growth [87]. Unfortunately, the majority of piezoelectric polymers, such as PVDF, PLLA, and PHAs are hydrophobic, and their surface hydrophobicity impedes sufficient cell adhesion [87,88]. To solve this problem, plasma treatment [66,89,90], chemical hydrophilic functionalization [5,54,57,89], or polymer blending [44,45,51,55] are routinely conducted for improving the hydrophilicity of piezopolymeric scaffolds. For example, Xia et al. [88] have proposed *in situ* hydrophilic modification of PLLA nanofibers for cell adhesion. Due to the electrostatic interaction between dopamine and PLLA nanofibers, an effective and robust *in situ* modification was obtained without compromising the nanofibrous structure [88]. Furthermore, the addition of chitosan decreases water contact angles (WCAs) of PHB from 125° to 43° for randomly aligned PHB/chitosan 80:20 fibrous scaffolds and from 111° to 33° for aligned ones [45,51]. Of note, greater fiber alignment is reported to enhance the hydrophilicity of electrospun scaffolds [45,51].

Nonetheless, the degradation rate of modified scaffolds can be accelerated by the increased hydrophilicity [45,88], which can actuate premature impairment of scaffolds' mechanical and piezoelectric performance. Therefore, it makes sense to find an optimal compromise between scaffolds' satisfactory hydrophilicity and prolonged integrity and electroactivity.

3. Effects of piezoelectric materials on cell behavior and tissue growth

As mentioned above, a scaffold's bioactivity plays a critical role in robust nerve regeneration. Various stimuli have been utilized in tissue engineering, among which, electrical stimulation is more effective for soft tissues such as skin, cardiac, and nervous tissue. Electric output can provide a distinctly favorable bioelectrical microenvironment [11,36], which is especially relevant for the nervous system. When a nerve defect is formed, the transmission of electrical signals is terminated [11]. Thus, it is reasonable to develop materials that can maintain electrical-signal

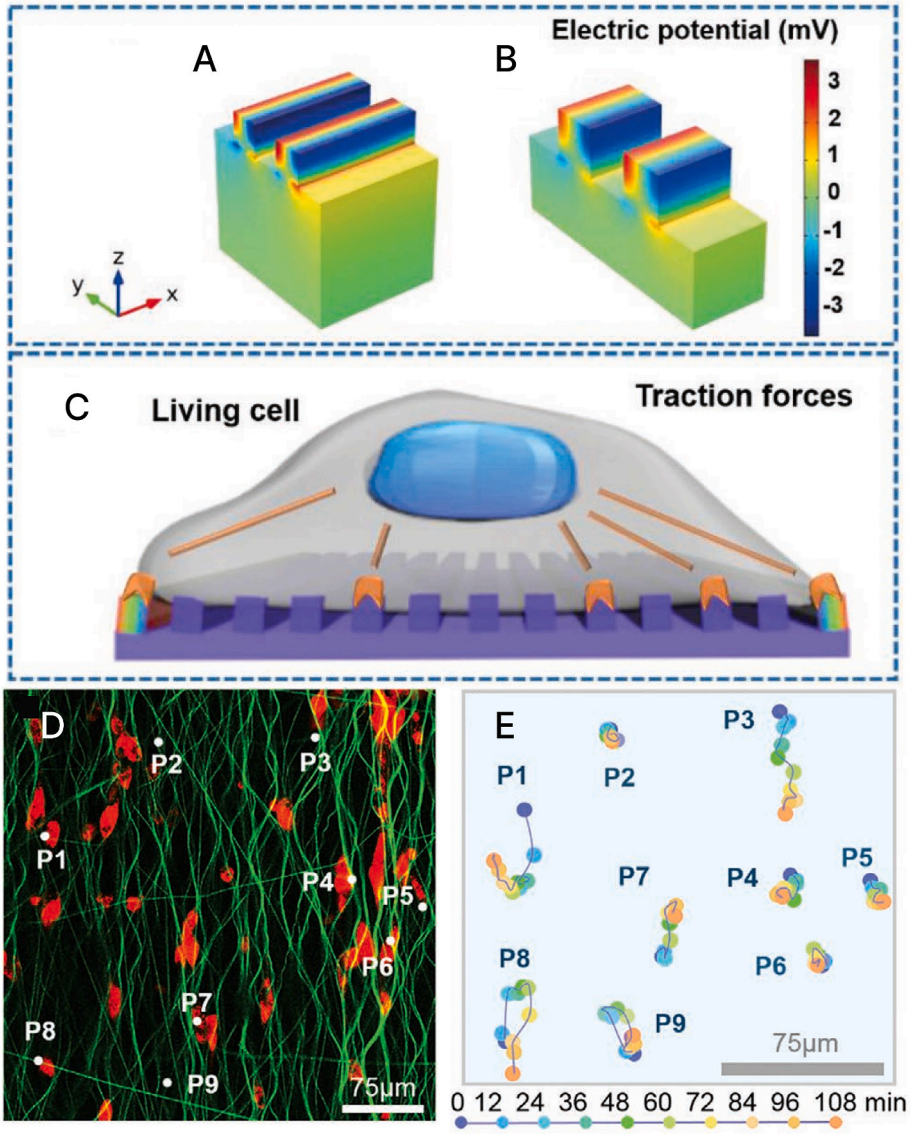

Fig. 2. Cell traction forces can induce the mechanical deformation of piezoelectric polymers and consequently piezoelectric potential. The PVDF nanostripes generated a voltage of 3.4 mV (200-nm nanostripes, A) and 2.93 mV (500-nm nanostripes, B) under a force of 10 nN. (C) Schematic of inherent cell forces of live cells grown on the piezopolymeric (PVDF) surface with nanoscale stripe arrays. Reprinted from Ref. [67] with permission from Wiley. (D) A fluorescence image of PVDF nanofibers (green, FITC) and cells (red, DiD Perchlorate). (E) Migration paths of nine random points of nanofibers within 108 min. Reprinted from Ref. [66] with permission from Wiley. Differentiation mechanisms of PC12 cells.

conduction and ensure electrical stimulation for nerve cells. Electrical stimuli can guide regenerating axons across the gap to connect the proximal and distal stumps of the injured nerve by biological signal transduction. For instance, neurons stimulated by an electric field of 50 mV mm^{-1} show greater neurite outgrowth and increased alignment in the direction of the electric field as compared to unstimulated neurons or cells exposed to a 10 or 100 mV mm^{-1} field [20]. The stimulation by the electric field of 50 mV mm^{-1} in coculture with SCs further boosts the neurite outgrowth [20]. A direct electric field can also enhance NSC activities [91]. It has been demonstrated that a population of neurons is 1.6 times larger—with longer neurites (73 vs. 108 μm)—for NSCs cultured on a cross-linked conductive PEDOT substrate under electrical stimulation [91]. Moreover, peripheral nerve regeneration in extended gaps has become possible via incorporation of electrical stimulation [26,92]. Zhang et al. [92] have proposed a magnetoelectric 3D matrix for remote and wireless electrical stimulation of nerve repair (Fig. 1). They prepared magnetoelectric core/shell Fe_3O_4@$BaTiO_3$ nanoparticles, which were subsequently loaded into hyaluronan/collagen hydrogels (Fig. 1A). In an external magnetic field, magnetoelectric Fe_3O_4@$BaTiO_3$ particles affected electrical potential of the extracellular environment, thus providing strong and robust stimuli for PC12 cell growth, Ca^{2+} influx, and expression of neural-cell proteins (Fig. 1B).

Conventionally, electrical signals are applied through a conductive scaffold and external power in an invasive manner [93]. Electrical stimulation generally requires auxiliary devices, such as electrodes, for generating electric fields [19,20,94]. Nonetheless, there are several drawbacks of this approach, such as i) the need for a complex circuit system with an external power source to implement electrical stimulation [20,26], ii) inflammation and gliosis caused by implanted electrodes [27], and finally iii) the necessity of a second surgical procedure to remove the electrodes. Moreover, energy storage capacity of batteries is limited, which hampers long-term use of such neurostimulators [28]. Accordingly, wireless and self-powered devices for nerve defect repair are arousing an interest. Unlike conventional electrical treatment, the use of piezoelectric polymers can provoke changes in a surface charge without external energy sources or electrodes [29–32]. Piezoelectric

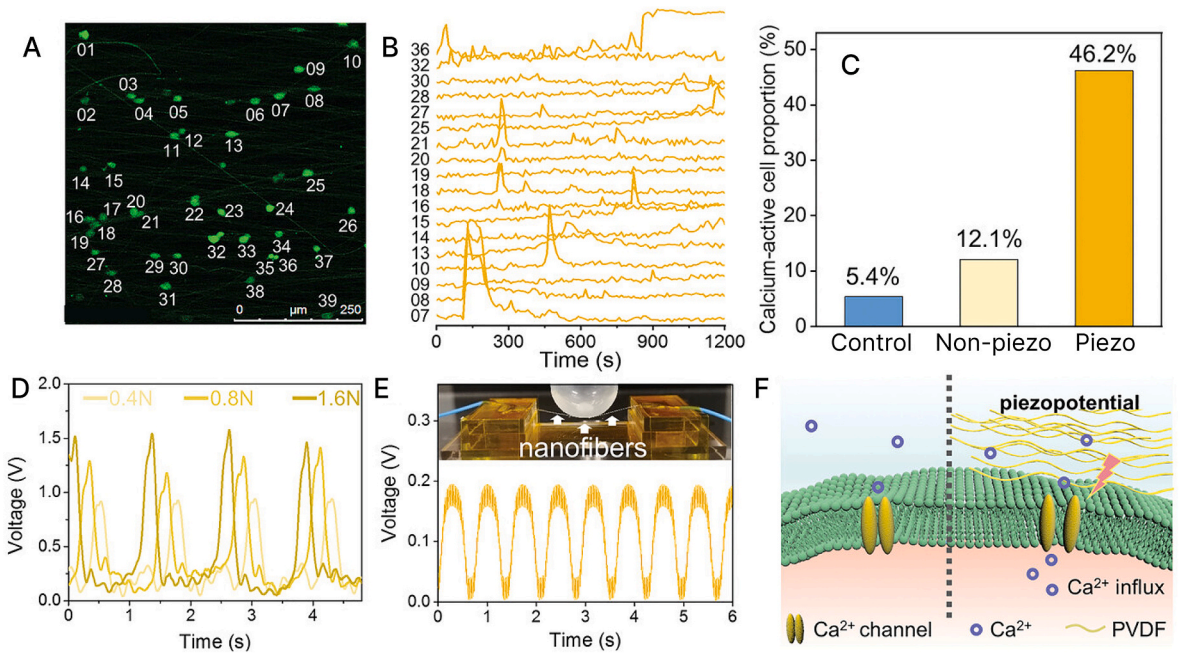

Fig. 3. Calcium influx is responsible for neuron regeneration and axonal development. (A) Intracellular calcium staining of rat bone marrow–derived stem cells (rBMSCs) on an electroactive scaffold. (B) Transient calcium activity of the cells on the electroactive scaffold. The numbers represent different cells in the field of view. (C) The proportion of calcium-active cells in different samples of substrates. (D) Output voltage of the piezoelectric scaffold under external forces of 0.4–1.6 N. (E) Output voltage of a bundle of nanofibers under periodical deformation along the *z*-axis. (F) An intracellular calcium transient caused by piezopotential. Left: Cells cultured on tissue culture plastic (TCP); right: cells cultured on the piezoelectric scaffold. Reprinted from Ref. [66] with permission from Wiley.

polymers can convert a mechanical force into electricity (direct piezoeffect) and vice versa (converse piezoeffect). Structural requirements for polymers to manifest piezoelectricity are (1) the presence of permanent molecular dipoles, (2) the ability to align or orient molecular dipoles, (3) the ability to sustain an alignment once it is achieved, and (4) the ability of the material to undergo large strains when mechanically stressed [95]. Piezoelectricity in polymers is the result of the reorienting of molecular dipoles within a bulk polymer; this phenomenon can be implemented through the application of a high electric field or stretching (drawing) [36].

In some articles, piezoelectric scaffolds have been shown to support the adhesion, growth, differentiation, and myelination of SCs as well as neurite extension [31,46–48]. Negative and positive surface charges generated by piezoelectric substrates have also been found to promote metabolic activity and maturation of neurons in primary culture [96]. Piezoelectric composite scaffolds promote proliferation and differentiation of PC12 cells [12,97,98]. Moreover, piezoelectric PVDF scaffolds may specifically enhance neuron-like differentiation of mesenchymal stem cells (MSCs), as indicated by the expression of neural and neurogliocyte makers and Tuj1 as well as by neurite length [66,67,99]. Furthermore, ultrasound-mediated piezopolymer/ceramic composite films are reported to improve the viability and differentiation of human neuroblastoma SH-SY5Y cells by promoting Ca^{2+} transients [68]. Piezoelectric nanofibers combined with ultrasound vibration enhance the expansion of NSCs without any growth factors [90]. As for *in vivo* studies, piezoelectric guidance channels have been successfully used to repair transected sciatic nerves in adult mice and rats and significantly promoted axonal myelination as well as electrophysiological, morphological, and functional nerve restoration, comparably to the current gold standard [31,69,100]. These effects are attributed to fields or charges generated by the piezoelectric conduits [69]. Furthermore, electroactive conduits have been shown to support SC survival, regeneration of sensory ($CGRP^+$) and brainstem ($D\beta H^+$) axons, extension of astrocyte/$GFAP^+$ processes, and blood vessel formation after complete spinal cord transection [101].

Piezoelectric capacity of such materials can be activated by macroscale body movements *in vivo* [29], changes in posture, or interstitial-fluid circulation, which may promote injury healing. In addition, the location of a piezoelectric implant in the body can affect the biological response owing to the extent of the anatomical deformation caused by random animal movements [102]. Desired deformations can be caused by cell attachment and migration *in vitro* (the so-called cell traction forces, Fig. 2C) [65–67,88] and the general locomotion of a tissue because cells have been shown to contract substrates by 1–3 μm [65]. Typically, the cell traction force is in the range of 0.1–10.0 nN [66,67]. Zhang et al. [67] have simulated the piezoelectric potential generated from cell motion on PVDF nanostriped arrays by applying a force of 0.1–10.0 nN at the top of the piezoelectric strip. As a result, the PVDF nanostripes generated a piezoelectric potential of 34 μV to 3.4 mV as cell traction forces increased from 0.1 to 10.0 nN (Fig. 2A and B). Liu et al. [66] have directly observed the cell traction–driven deformation of piezoelectric nanofibers under a fluorescence microscope. Judging by time-lapse confocal imaging, there was obvious cell migration and nanofiber displacement, indicating that the PVDF nanofibers were deformed by 5–60 μm within 108 min (Fig. 2D and E), thereby generating piezopotential of approximately 98 μV to 18 mV to stimulate stem cells [66]. Although piezoelectric materials activated by cells' and body movements have produced positive outcomes [29,65–67,88,102], stimuli controllability of these stimulators is rather poor. Electrical parameters offered by these self-powered scaffolds, such as current density, pulse width, stimulation frequency, and operation timeliness, cannot be well controlled on demand [28]. To address this limitation, a piezoelectric effect can be artificially promoted by alternative techniques such as noninvasive ultrasonication [28,90,99,103] (known for its deep tissue penetration and good clinical safety) or magnetic fields [92]. A drawback of the ultrasound treatment is strong absorption of sound waves by tissues, resulting in tissue heating. In this regard, a promising alternative is magnetoelectric materials in which the piezoelectric response is activated via polarization owing to magnetostriction of magnetic particles when exposed to a magnetic field [92,104–106]. For instance, PVDF/barium titanate ($BaTiO_3$) composites are becoming increasingly attractive in tissue engineering. In a comprehensive study

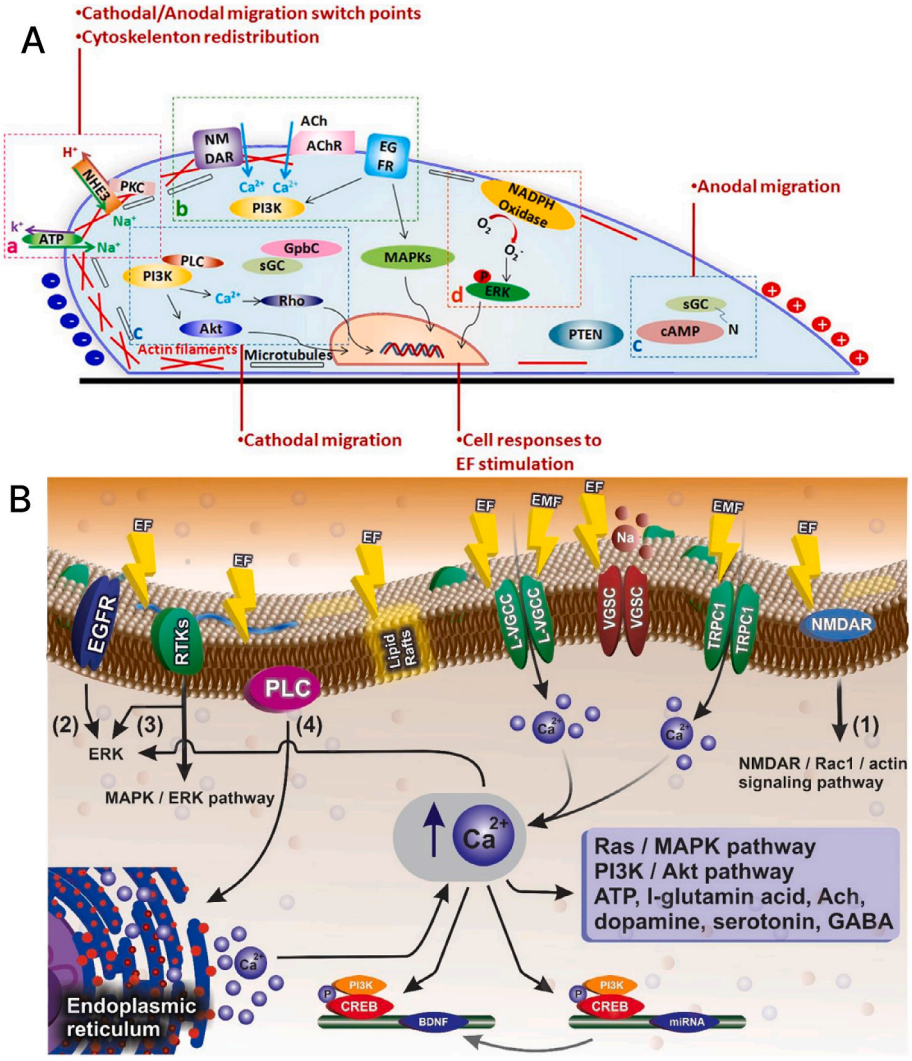

Fig. 4. Effects of piezoelectric stimulation on neural cells. (A) The signaling network in electric-field–stimulated cells. (a) Ion channels NaKA and NHE3. EF: electric field. (b) AChR and NMDAR are activated at the cathodal pole; EGFR activates downstream MAPKs and PI3K. (c) PI3K at the leading edge launches other pathways via AKT or merges with PLC to stimulate Rho via Ca^{2+}. Cathodal and anodal cell migration are mediated by the catalytic domain of sGC and the N domain of sGC along with cAMP, respectively. (d) Other biomolecules involved in the signal transduction during electric-field stimulation, i.e., NADPH and ERK. Reprinted from Ref. [109] with permission from Elsevier. (B) Reformation of cytoskeletal filaments and polarization of lipid raft structures. (1) An NMDAR ligand triggers the NMDAR–Rac1–actin pathway. (2) EGFR activation, followed by ERK signaling. (3) The MAPK–ERK pathway and ERK phosphorylation via RTKs. (4) Upregulation of intracellular Ca^{2+} from the endoplasmic reticulum; phosphorylation-dependent activation of CREB; binding of phospho-CREB to microRNA and the expression of BDNF. Reprinted from Ref. [2] with permission from Elsevier. (C) NGF-induced differentiation via the TrkA–Ras–MEK–ERK pathway. (D) The differentiation pathway induced by piezoelectric depolarization of the PC12 cell membrane, i.e., the cAMP-dependent pathway. Reprinted from Ref. [103] with permission from Nature.

[105], Ag-decorated $BaTiO_3$ nanoparticles were introduced into a PVDF scaffold, which promoted cell proliferation and differentiation *in vitro* owing to enhanced electric output. A wireless electrical stimulation system was constructed in Ref. [106] by taking advantage of the magnetoelectric coupling effect. Specifically, piezoelectric $BaTiO_3$ was *in situ*–grown on magnetostrictive $CoFe_2O_4$, forming nanoparticles with core–shell structure, which were subsequently incorporated into polymer scaffolds. The *in vitro* results indicated that the electrical signals effectively promoted cell proliferation and differentiation and upregulated some genes' expression [106]. Nonetheless, applications of magnetoelectric materials are limited in the field of nerve reconstruction and require further technological advances.

4. Mechanisms by which piezoelectric materials regulate cell behavior

The mechanism by which piezoelectric scaffolds promote nerve tissue regeneration is rather complex and may involve multiple phenomena. The reason behind successful piezoelectric stimulation of nerve regeneration is the inherent electric properties of neural cells. The membrane of neural cells is negatively charged on the inside and positively on the outside [2]. Therefore, even in the absence of neural transmittance, there exists resting membrane potential on the order of −70 mV. The purpose of the resting potential is the transport of sodium and potassium ions through the neural-fiber membrane and potassium channels, respectively. Electrical activity is mediated by the action potential, which is a random increase of resting potential in response to exterior electrical impulses, followed by rapid depolarization and repolarization. Because of these potentials and ion flows, cellular behavior can be controlled by electrical stimulation. Proper patterns of the stimulation can direct neural cell growth and regeneration [107].

Calcium influx is responsible for neuron regeneration and axonal development after an injury [92,108]. Alterations of intracellular calcium concentrations trigger downstream effectors that adjust the

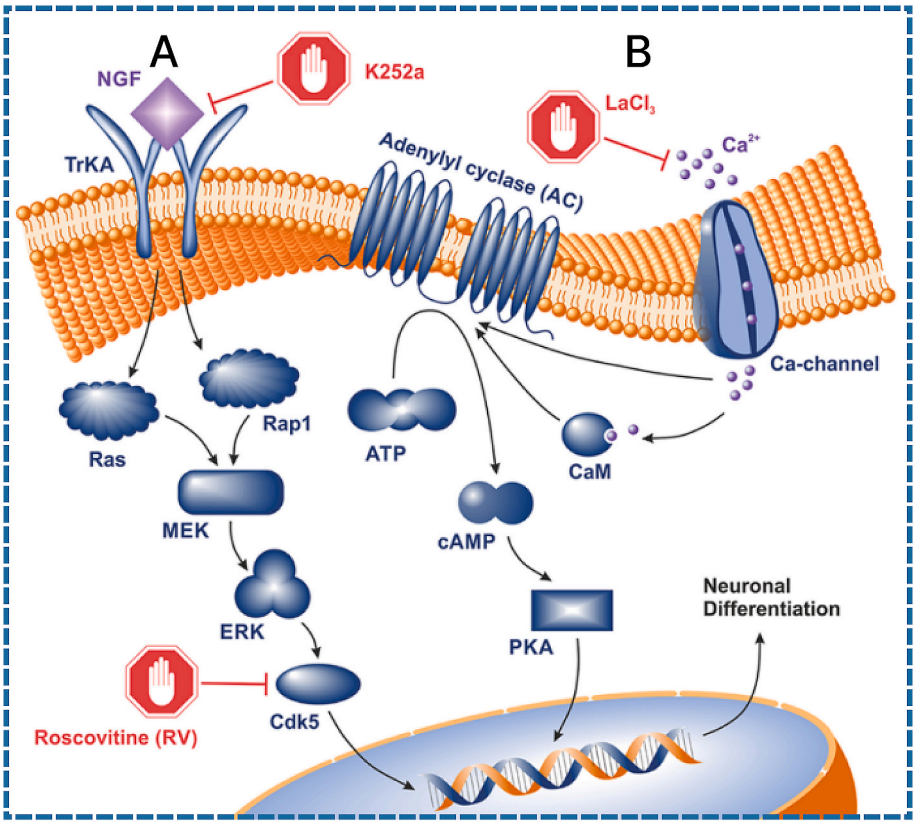

Fig. 5. (A) NGF-induced differentiation via the TrkA–Ras–MEK–ERK pathway. (B) The differentiation pathway induced by piezoelectric depolarization of the PC12 cell membrane, i.e., the cAMP-dependent pathway. Reprinted from Ref. [103] with permission from Nature.

regeneration. Such ion variation induces bioelectricity generation at the cellular level. Transmembrane calcium channel activation and intracellular calcium transients play important roles in the regulation of stem cell fate. Liu et al. [66] monitored intracellular Ca^{2+} concentration over time (Fig. 3A and B) when cells were cultured on a piezoelectric scaffold and found 46.2 % of the cells showing obvious transient calcium activity within 1200 s, and this percentage was 3.82-fold and 8.56-fold higher than that on nonpiezoelectric substrates (Fig. 3C). The generated piezopotential (Fig. 3D and E) was able to activate transmembrane calcium channels, allowing an influx of extracellular Ca^{2+} into the cytoplasm (Fig. 3F).

Piezoelectric stimulation polarizes signaling ingredients, thereby causing asymmetric initiation of signaling ingredients and of the downstream cytoskeleton, and thus guides cell movement in the electric field (Fig. 4A) [109]. Cathodal/anodal movements are activated by ion channels NaKA and NHE3 (Fig. 4A, *a*). During electric-field exposure, NaKA and NHE3 accumulate at the cathodal/anodal edge of the migrating cell. Such activation involving Na^{+} and Ca^{2+} influxes creates an ion gradient along/against the electric field, thereby causing depolarization of the cell and a redistribution of the cytoskeleton. NHE3 induces the cytoskeleton redistribution via a complex with PKC and tubulin in an applied electric field. Receptors on the plasma membrane implement ion influxes and trigger signaling during electric-field exposure, where AChR and NMDAR are activated at the cathodal pole of the electric field affecting the Ca^{2+} influxes and cell depolarization (Fig. 4A, *b*). By contrast, epidermal growth factor receptor (EGFR) that is activated by the electric field triggers downstream MAPKs and PI3K. The PI3K–AKT signaling pathway (Fig. 4A, *c*) strongly influences electrotaxis: PI3K and downstream effectors accumulate at the leading edge of an electrotaxing cell and launch other pathways via AKT or merge with phospholipase C (PLC) thus stimulating Rho via Ca^{2+}. PTEN is downregulated at the cathodal pole and has higher activity at the anodal pole (Fig. 4A, *c*). The catalytic domain of soluble glucocerebrosidase (sGC) contributes to cell migration to the cathode side, while the N domain of sGC and cyclic adenosine monophosphate (cAMP) facilitate the movement toward the anode. An electric field can activate NADPH oxidase, promoting phosphorylation of ERK (Fig. 4A, *d*).

Furthermore, piezoelectric stimulation causes the reformation of the cytoskeletal filaments and polarization of lipid raft structures (Fig. 4B). Piezoelectric stimulation alters the N-methyl-d-aspartate receptor (NMDAR) ligand gate and triggers NMDAR–Rac1–actin signaling cascade (Figs. 4B, *1*). Electrical stimulation also triggers EGFR, followed by ERK signaling (Figs. 4B, *2*). The MAPK–ERK pathway and ERK phosphorylation are initiated via tyrosine phosphorylation in receptor tyrosine kinases (RTKs) (Figs. 4B, *3*). Concentration of intracellular Ca^{2+} (coming from the endoplasmic reticulum) is increased by PLC activation (Fig. 4B, *4*). Ca^{2+} influx through voltage-gated Ca^{2+} channels or expression of transient receptor potential canonical 1 (TRPC1) stimulates the phosphorylation of a transcription factor, e.g., cAMP response element-binding protein (CREB). The accumulation of Cav1-dependent CREB phosphorylation at Ser133 promotes expression of neuronal genes (*NeuroD1* and neurogenin 1) and recruits histone acetyltransferase CBP. Phospho-CREB can also regulate the expression of microRNAs (via a promoter) and BDNF. Upregulation of genes of BDNF and of its receptor TrkC in motor neurons corresponds to acceleration of axonal regeneration [3,110]. Alterations of cytoplasmic Ca^{2+} levels affect the generated ATP, L-glutamic acid, acetylcholine, dopamine, serotonin, and GABA concentrations. The electrical stimulation not only affects the formation of neuromuscular junctions by altering ion flux across the plasma membrane, thereby controlling membrane potential and signal transduction pathways [111], but also enhances cell proliferation and migration [17].

In addition to the electrosensitive nature of neural cells, many extracellular and cytoplasmic biopolymers, including ubiquitous

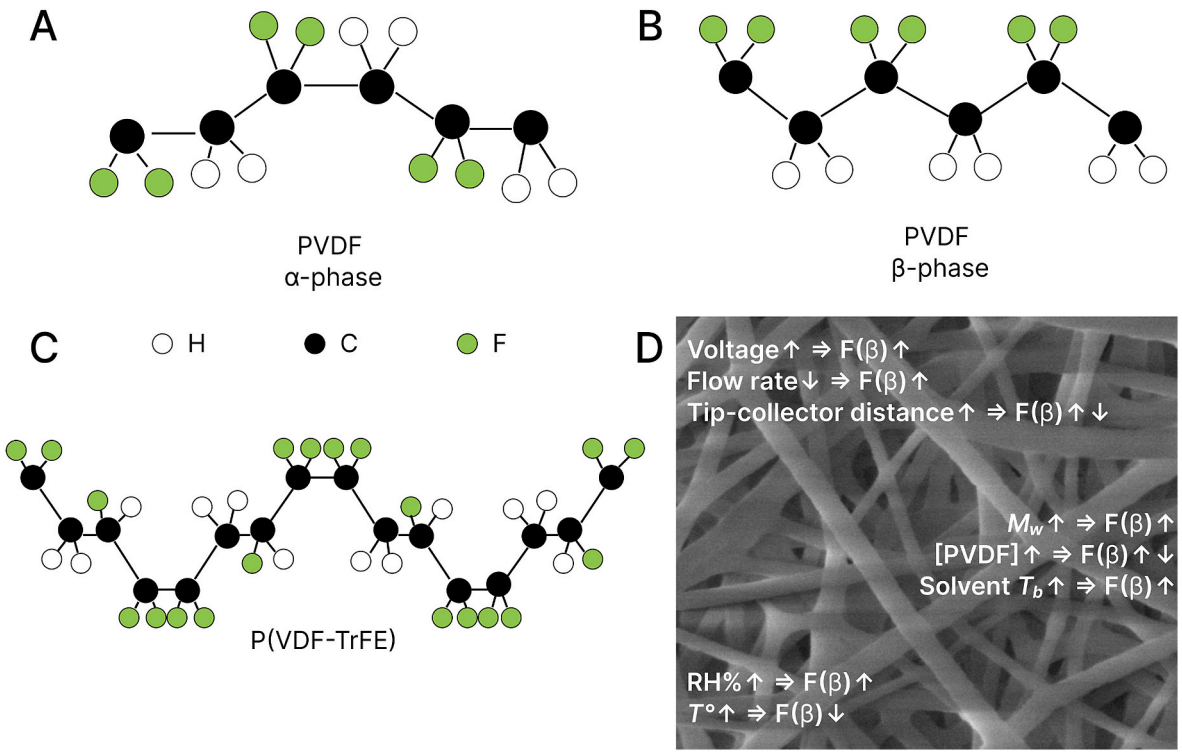

Fig. 6. Macromolecular structure of PVDF. (A) Structure of randomly oriented PVDF chains constituting the nonpiezoelectric α-phase. (B) PVDF chains' polarized orientation induced by stretching or high-voltage poling resulting in the emergence of the piezoelectric β-phase. (C) Chain confirmation of P(VDF-TrFE). (D) The influence of electrospinning parameters, solution, and environment on β-phase formation. M_W: molecular weight, RH%: relative humidity. Adapted from Ref. [71] with permission from MDPI.

polypeptides (e.g., collagen and many enzymes) and polynucleotides (e.g., RNA and DNA), possess piezoelectric or charge storage capabilities [10,69]. These properties play an important part in tissue growth and remodeling owing to intersecting electrical, mechanical, and chemical activities. It is possible that the primary purpose of the piezoelectricity associated with these biopolymers is to alter their conformation or orientation through electroconformational coupling mechanisms, and thereby to enhance enzyme-driven reactions [112]. It is also possible that the piezoelectric capacity of biopolymers is responsible for greater synthesis or secretion of ECM molecules [113], which may induce neurite outgrowth. Moreover, the growth cone at the leading edge of a neurite may serve as an electric-field sensor that transmits growth signals to the nucleus via secondary-messenger systems [114]. Electroactivity of piezoelectric polymers may complement the distinct electrical environment characteristic of the nervous system. Furthermore, electrical stimulation by polymeric substrates can result in the adsorption of positive charges and ECM molecules onto the polymeric chains [115]; this phenomenon also boosts neural regeneration. It has also been proposed that the piezoelectric effect may (1) facilitate the migration, proliferation, and differentiation of SCs; (2) promote the secretion of nerve growth factors (NGFs) by SCs; and (3) have a chemotactic influence on tubulin and microfilaments in axons [31]. Meanwhile, the electric potential generated by piezoelectric scaffolds has been found to enhance angiogenesis, which further contributes to nerve restoration [31].

Recently, a molecular mechanism underlying the promotion of neuron-like PC12 cell differentiation by piezoelectric stimulation was investigated (Fig. 5) [103]. The well-known differentiation induced by NGF (Fig. 5A) occurs as follows: NGF molecules bind to RTKs (TrkA), causing intracellular phosphorylation; the activation of Ras or Rap1 initiates downstream signaling cascade MEK→ERK→Cdk5 promoting neuronal differentiation of PC12 cells. On the contrary, the PC12 differentiation induced by piezoelectric stimulation (Fig. 5B) implies the activation of calcium channels in the cell, thereby causing an increased Ca^{2+} influx. An elevated intracellular Ca^{2+} concentration activates adenylyl cyclase, which promotes the conversion of ATP to cyclic AMP (cAMP). Subsequently, cAMP launches the protein kinase A (PKA)-dependent neuronal differentiation pathway. Zhang et al. [99] have speculated that the local electrical signals generated by piezoelectric membranes may be transmitted to the intracellular environment through direct contact between the material and cells. These signals may promote the expression of related genes, which in turn should induce neural differentiation of stem cells.

5. Types of piezoelectric polymer materials applied to neural tissue engineering

5.1. Pure PVDF scaffolds

PVDF is the best-studied piezoelectric polymer and has a piezoelectric coefficient of 20 pC/N [95]. Polar polymers, such as PVDF, are ferroelectric and exert a piezoelectric effect after poling treatment [36]. Fig. 6A and B presents the process of reorienting of molecular dipoles in PVDF. Five crystal phases, namely α, β, γ, δ, and ε, have been identified in PVDF, and α- and β-phases are the most commonly utilized [116]. In the α-phase, the chains are packed in the unit cell so that the molecular dipoles are antiparallel, resulting in nonpolar crystal structures (Fig. 6A). The β-phase has the most pronounced piezoelectric properties because all the dipoles are parallel and contribute to the largest dipole moment per unit cell (Fig. 6B) [117].

P(VDF-TrFE) is the best-known and most investigated PVDF copolymer, which is synthesized by polymerization of vinylidene fluoride (VDF) and trifluoroethylene (TrFE). The phase configuration and phase transformation of P(VDF-TrFE) (Fig. 6C) are very similar to those of PVDF (Fig. 6A and B). Unlike PVDF, P(VDF-TrFE) always contains the ferroelectric β-phase because the addition of the third fluoride into the

Table 2
A summary of neat PVDF and P(VDF-TrFE) scaffolds and conduits for neural tissue engineering.

Scaffold (conduit) material	Scaffold fabrication and characterization	Piezoelectric performance	Biological model	Outcome	Ref.
In vitro					
PVDF, P (VDF-TrFE)	Solvent-cast films	2–3 mV at 1200 Hz	Nb2a cell differentiation	Enhanced neural differentiation for up to 96 h on piezoelectric substrates compared to electrically neutral ones	[122]
P(VDF-TrFE)	Electrospun aligned scaffolds	The max and the avg current were 1.75 and 0.76 nA, respectively	SCs and fibroblasts	Scaffolds of various thicknesses promoted the adhesion and alignment of SCs and fibroblasts	[46]
P(VDF-TrFE)	Electrospun conduits with aligned fibers with diameters of 791 ± 19 nm, impregnated with a decellularized extracellular matrix (dECM). The conduit porosity and modulus were 52.5 % ± 1.2 % and 57.91 ± 6.12 MPa, respectively	Current amplitude of ~9 nA upon a 0.2 cm deformation	SCs and fibroblasts	Cells got integrated into a 3D scaffold and assembled a robust ECM. Cells elongated in the direction of the aligned fibers	[47]
P(VDF-TrFE)	Electrospun scaffolds with aligned 1.5-μm fibers	Not reported	SCs	The scaffolds supported SC growth, myelination, and neurite extension	[48]
P(VDF-TrFE)	Randomly oriented and aligned annealed electrospun scaffolds with average fiber diameters of 750 nm to 3.6 μm	Not reported	DRG neurons	Elevated adhesion and neurite extension on PVDF fibrous scaffolds compared to the cast films. The greatest neurite length on micron-sized annealed aligned scaffolds in comparison with randomly oriented fibrous mats	[65]
PVDF	Electrospun scaffolds with different fiber alignments and fiber diameters of ~1.5–2 μm. The porosity of nonaligned and highly aligned scaffolds was 86 % and 46 %, respectively	Not reported	Monkey NSCs' growth and differentiation	Nonaligned PVDF scaffold favored both NSC maintenance and glial differentiation, whereas weakly aligned PVDF was the most appropriate for neuronal differentiation. The highly aligned fibrous mats sustained neuronal differentiation of NSCs, while having a negative impact on glial differentiation	[70]
P(VDF-TrFE)	Randomly oriented and aligned electrospun scaffolds with average fiber diameters of 750 nm to 3.3 μm. Annealing improved the porosity of the randomly oriented scaffolds from 51 % to 74 %	Piezoelectric properties were enhanced after annealing as shown by an increase in the β-phase content and crystallinity	Differentiation of hNSCs/NPCs	Annealed and aligned microfibrous scaffolds were the most efficient for neural differentiation, as evidenced by neurite lengths and gene expression levels. These scaffolds facilitated the formation of mature neural cells exhibiting neuron-like characteristics	[49]
PVDF	The poled β-PVDF membrane with a thickness of 25–30 μm.	$d_{33} = -30 \pm 2$ pC/N	PC12 cell differentiation	The effect of piezoelectric stimulation on neural differentiation was comparable to that of neuronal growth factor (NGF)	[86]
PVDF	Randomly oriented and aligned electrospun networks with the average fiber diameter of 200–300 nm. The β-phase content was improved by annealing. Young's moduli of an individual PVDF nanofiber and a-PVDF nanofibrous film were 1.12 GPa and 3.4 kPa, respectively. Oxygen plasma treatment reduced the WCA of the PVDF nanofibers from 123–132° to 52–72°	d_{33} was −24 pC/N (a-PVDF) and −13 pC/N (r-PVDF). Piezopotential was in the range from 98 μV to 18 mV	rBMSCs	More cells on a-PVDF than on r-PVDF or TCP at days 3 and 5. Annealed aligned fibrous mats (a-PVDF) efficiently promoted cellular differentiation. The neurites' average length on a-PVDF was 91 μm, which was much longer than that on the r-PVDF scaffold (68 μm)	[66]
PVDF	Films with distinct stripe arrays were replicated from homostructural silicon molds. The sizes of the individual stripes were 200 and 500 nm. Then, the films were thermally annealed. The β-phase proportion in the films as determined by FTIR was 0.47–0.54	P_r and P_s were 42 and 55.7 mC/m^2, respectively[a]	rBMSCs	Topography played a crucial role in cell adhesion and proliferation rather than in piezoelectricity. Meanwhile, piezoelectricity rather than the nanotopography of the stripe array enhanced neuron-like differentiation	[67]
PVDF	Solvent-cast films. Surface potentials of positively and negatively charged films were 6 V and −4 V, respectively	d_{33} of −24 pC/N	Rat neurons in primary culture	Negatively charged PVDF film promoted cell metabolism and maturation 1.7 times better than electrically neutral PVDF did	[96]
In vivo					
P(VDF-TrFE)	Heat-melt extrusion followed by high-voltage corona poling	Polarization of 150 pC/cm^2 upon a 0.2 mm deformation	Rat sciatic nerve defect (10 mm)	A significantly greater number of myelinated axons as compared to the unpoled conduit group at 4 weeks postimplantation. Nerves regenerated successfully throughout only 50 % of each conduit owing to the lack of permeability in the rigid melt-extruded conduits	[69, 100]
P(VDF-TrFE) filled with SCs	Electrospun conduits with fiber diameters of 548 ± 139 and 711 ± 222 nm (for aligned and randomly aligned conduits, respectively) and a porosity of ~87–88 %.	Not reported	Rat spinal cord injury	Both conduits supported (i) SC survival, (ii) regeneration of sensory (CGRP$^+$) and brainstem (DβH$^+$) axons across the spinal cord/conduit interface, (iii) extension of astrocyte/GFAP$^+$ processes into the conduit, and (iv) blood vessel formation	[101]

[a] P_r is remnant polarization; P_s is saturated polarization.

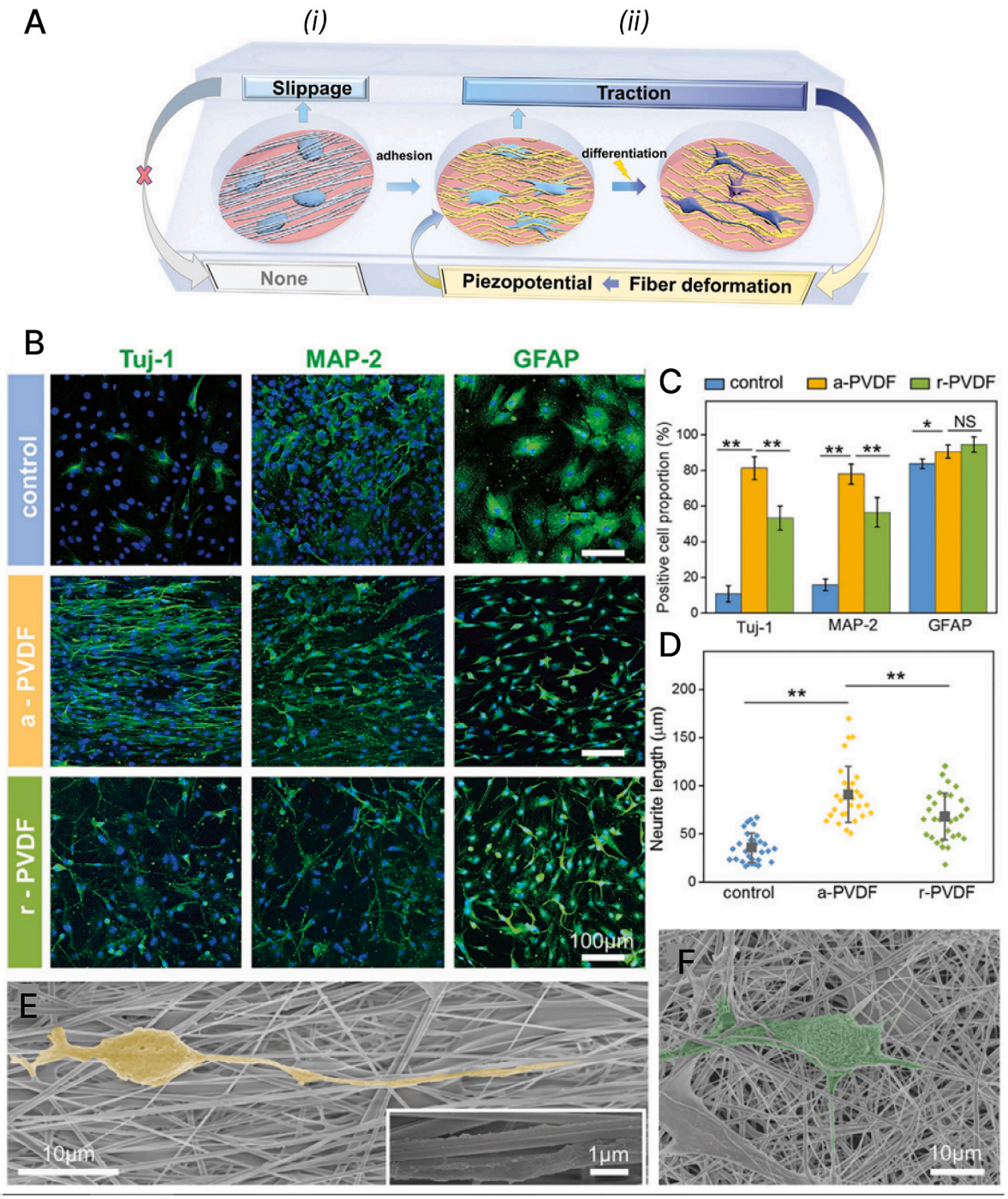

Fig. 7. Cell traction–actuated electrical stimulation of neural differentiation. (A) Stages of cell adhesion: *(i)* slippage, wherein cell activity does not cause nanofiber deformation; *(ii)* traction, which involves transmission of the intracellular biophysical signal to the exterior via integrin-mediated force transduction thereby deforming the fibrous network. (B) Immunofluorescent staining of neural makers Tuj1 and MAP2 and of neurogliocyte-specific maker GFAP after 7 days of differentiation of rBMSCs on PVDF nanofibrous mats. Cell nuclei are stained with DAPI (blue), whereas Tuj1, MAP2, and GFAP are immunostained (green). (C) Statistical analysis of the percentages of Tuj1-, MAP2-, and GFAP-positive cells. (D) Statistical analysis of neurite length of cells on different scaffold samples after 7 days of differentiation. (E–F) Representative scanning electron microscopy (SEM) images of the cells on a-PVDF (E) or r-PVDF (F) after 7 days of the differentiation. Error bars: mean ± SD. *$p < 0.05$, **$p < 0.01$; "NS" denotes no significant difference. Reprinted from Ref. [66] with permission from Wiley.

TrFE monomer unit with a large steric hindrance favors the all-*trans* conformation, generating the ferroelectric β-phase regardless of the processing method used [118]. Compared to PVDF, P(VDF-TrFE) has higher crystallinity and a preferred orientation of good growth crystallinity, which improves the electromechanical coupling factor [118]. As a consequence, P(VDF-TrFE) possesses piezoelectric coefficient d_{33} of 38 pC/N [118], which is one of the highest among polymers.

PVDF and P(VDF-TrFE) can help to regenerate different types of tissues, including bone [119], skin, cartilage, and a tendon [95] as well as nerves [46–48]. Numerous reports suggest that the copolymer is cytocompatible and exerts a positive influence on cell adhesion and proliferation [119,120]. Moreover, electrospun P(VDF-TrFE) fibers can stimulate the differentiation of cells into a mature phenotype and thus promote stem cell–induced tissue repair [121]. Table 2 summarizes

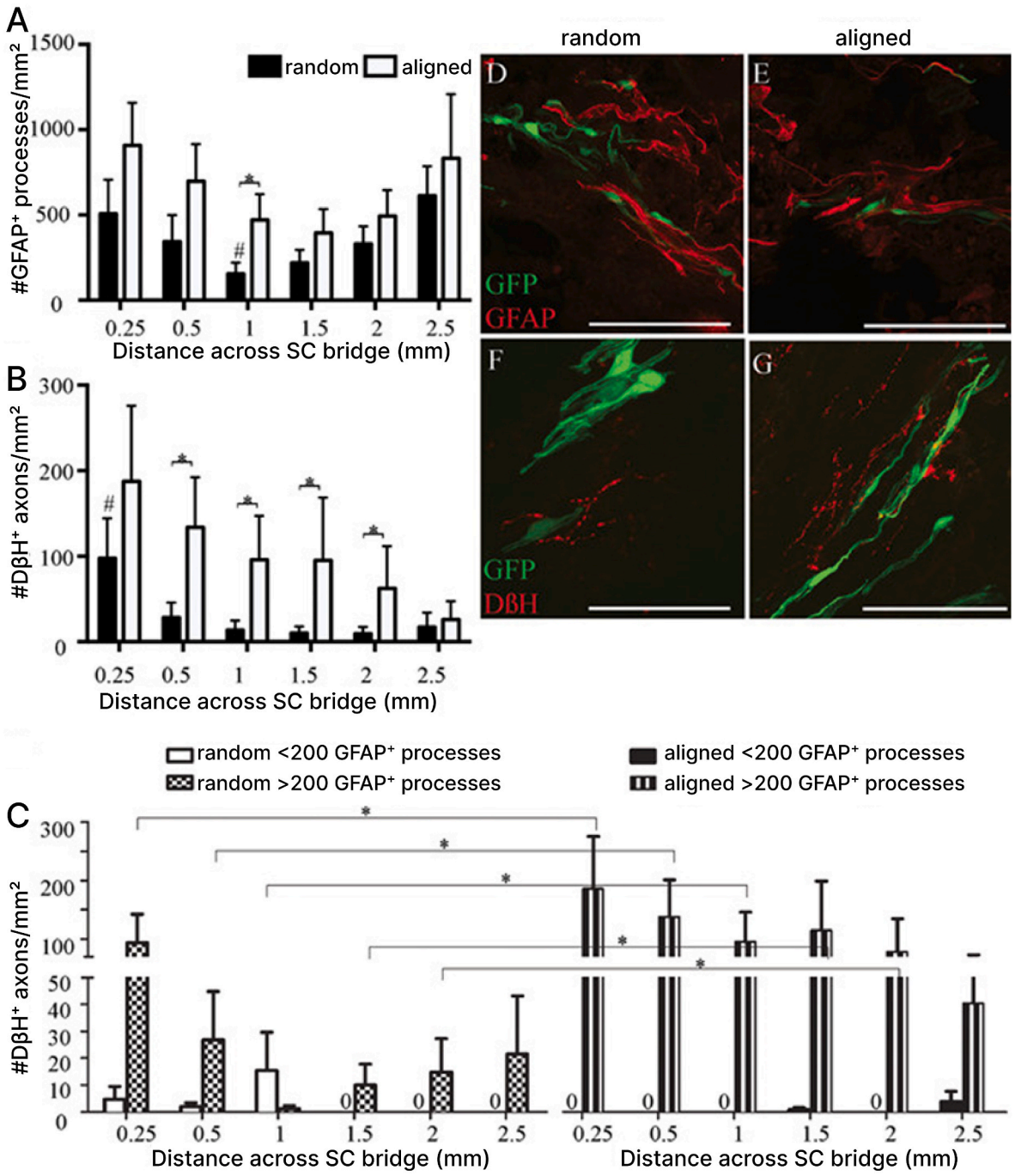

Fig. 8. Nerve regeneration by SC-filled P(VDF-TrFE) conduits after complete spinal cord transection. Numbers of immunostained GFAP$^+$ processes (A) and DβH$^+$ axons (B) at various distances from the rostral interface. Numbers of DβH$^+$ axons in randomly aligned vs. aligned fibrous conduits during a comparison of SC implants containing less or more than 200 GFAP$^+$ processes (C). Confocal fluorescence images of GFAP$^+$ processes and GFP-expressing SCs at the rostral interface of randomly aligned (D) or aligned (E) fibrous conduits. Confocal fluorescence images of DβH$^+$ axons colocalized with GFP-expressing SCs in randomly aligned (F) or aligned (G) fibrous conduits at 0.25 mm caudal to the rostral interface. Scale bars: D–G, 50 μm. Reprinted from Ref. [101] with permission from Wiley.

piezoelectric neural tissue engineering scaffolds composed of the PVDF polymer or P(VDF-TrFE) copolymers. Lee et al. [65] were the first to investigate the compatibility of neural cells with electrospun piezoelectric scaffolds having different fiber size and orientation. In that work, dorsal root ganglion (DRG) neurons attached to all fibrous scaffolds, and the behavior of the DRG was strongly affected by the scaffold design and fiber dimensions and orientation. Neurite length was the greatest on micron-sized annealed well-aligned P(VDF–TrFE) scaffolds in comparison with randomly aligned fibrous mats. Those authors stated that cell adhesion to piezoelectric materials might be due to integrin binding to ligands adsorbed onto the polarized negatively charged surface. Matrix sensing and deformation by the cells are mediated by focal adhesion complexes that integrate the matrix with the actin cytoskeleton.

Biomimetic materials with time-modulated properties (i.e., 4D biomimetic materials) have received growing attention due to their bionic nature. 4D biomaterials can be based on piezoelectric polymers and can create a dynamic cell microenvironment. For instance, Liu et al. [66] have fabricated aligned (a-PVDF) and randomly oriented (r-PVDF) electrospun nanofibrous networks and demonstrated a dynamic

Table 3
A summary of composite PVDF- and P(VDF-TrFE)-based devices for neural tissue engineering.

Piezopolymer material	Additives	Preparation technique	The additives' roles	Piezoelectric performance	Biological model	Key outcomes	Ref.
In vitro							
PVDF	MCM41; PAG	Incorporation of chopped electrospun nanofibers into gellan/PAG nanocomposites	MCM41 (15 wt%) enhanced piezoelectric properties and Young's modulus of PVDF nanofibers. PAG (2 wt%) raised scaffold conductivity to 12×10^{-5} S/cm	Output voltage of 230 mV	PC12 cells	Promoted cell growth with physicochemical benefits for neural cells	[97]
PVDF	PCL; gelatin/chitosan hydrogels; PAG; ZnO	Co-electrospinning; freeze-drying	ZnO and PAG increased conduit piezoelectricity. PAG gave high conductivity of 8.9×10^{-5} S/cm. The composite conduit could degrade by 5 % after 21 days *in vitro* due to the presence of PCL, gelatin, and chitosan. Chitosan/gelatin hydrogels turned the conduit hydrophilic	Output voltage of 1000 mV	PC12 cells	Elevated cell viability and proliferation	[12]
PVDF	FeOOH nanorods	Hydrothermal assembly of FeOOH on the surface of PVDF electrospun nanofibers	A release of Fe^{3+} into a culture medium	Piezoelectric potential of 2 V	rBMSC differentiation	Accelerated neural differentiation under ultrasonication proved by upregulated neural-cell–specific genes in the cells cultured on FeOOH/PVDF compared to cells on TCP during the same treatment	[99]
P(VDF-TrFE)	Barium titanate nanoparticles (BTNPs)	Cast/annealing	BTNPs increased surface root mean square (RMS) roughness (from 63 to 212 nm) and the β-phase content. Ultimate tensile strength and elongation at break of P(VDF-TrFE) diminished due to the defects (i.e., BTNPs) in the polymeric matrix	d_{31} was 53.5 and 11.8 p.m./V for P(VDF-TrFE)/BTNP and P(VDF-TrFE), respectively	SH-SY5Y cell differentiation	Elicited Ca^{2+} transients and enhanced cell differentiation and neurite elongation upon ultrasonic stimulation	[68]
P(VDF-TrFE)	$CoFe_2O_4$ (CFO)	Dip-coating followed by laser ablation	CFO served as a magnetic actuator for maneuvering	Not reported	PC12 cell differentiation	The piezopolymer matrix induced neuronal differentiation of PC12 cells, when subjected to ultrasonication	[98]
In vivo							
PVDF	PCL	Cast/annealing-solvent displacement	Improved mechanical properties, biocompatibility, and biodegradation: PVDF/PCL lost up to 9.1 % of mass after 4 months *in vivo*	d_{33} of 13.2 p.m./V	15-mm rat sciatic nerve (at 4 months)	PVDF/PCL scaffolds had an SFI of −27.7 %, which was significantly higher than that of the PCL group (−41.5 %)	[31]
PVDF	BZT-BCT@PDA	Electrospraying	BZT-BCT@PDA (50 wt%) enhanced piezoelectric performance of PVDF	Output voltage of 13.5 V	Rat sciatic nerve	Direct electrical neurostimulation was successfully achieved	[28]
PVDF/PLCL	SF/PEDOT cryogel	Solvent-casting; gradient freezing	High ductility of the PVDF/PLCL film with the elongation over 350 % due to PLCL. High conductivity (2.446×10^{-3} S/cm) of the SF/PEDOT cryogel	Amplitude of ~500 p.m. with bias voltage of 12 V (d_{33} was not reported)	SCs; PC12 cells; rat sciatic nerve (12 weeks)	Promoted proliferation and myelination of SCs and neuronal differentiation of PC12 cells. Facilitated peripheral nerve regeneration and functional recovery, comparable to those of an autograft	[11]
SF/poly (vinylidene fluoride-*co*-hexafluoropropylene) (PVDF-HFP)	$Ti_3C_2T_x$ (MXene)	Electrospinning	MXene enhanced piezoelectric and mechanical properties and antibacterial activity	Output voltage of up to 100 mV	SCs; rat sciatic nerve injury	Enhanced axonal elongation and myelination *in vivo* under ultrasound exposure. Recovery of motor and sensory function in rats	[125]

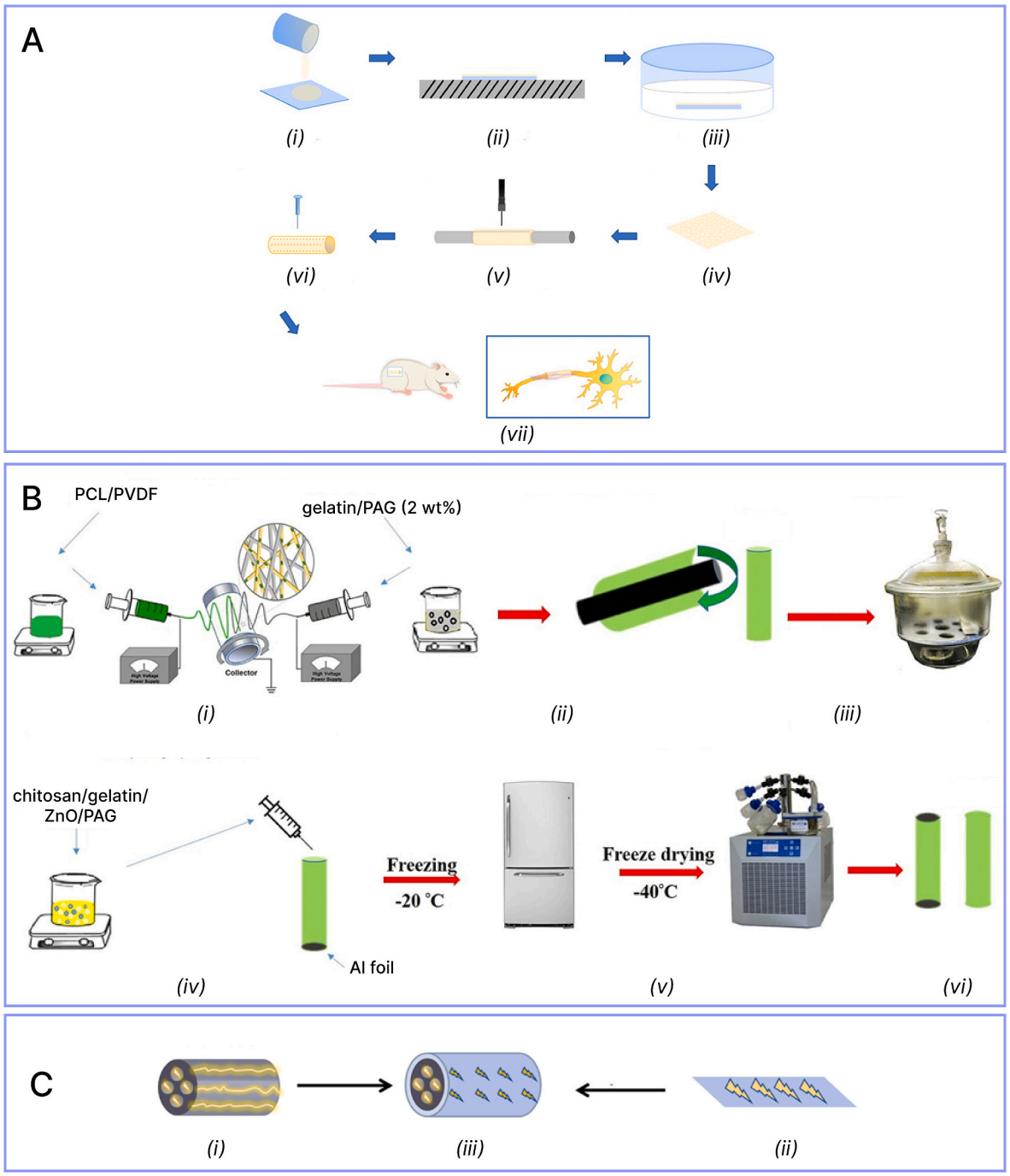

Fig. 9. Fabrication of composite PVDF-based conduits. (A) Fabrication of PVDF/PCL NGCs. *(i)* Casting on a glass mold. *(ii)* Annealing at 55 °C for 12 h *(iii)* Immersing in an ethanol bath. *(iv)* Drying in vacuum. *(v)* Rolling around a cylindrical model with a heat sealing process. *(vi)* Making of microporous structures by means of needles. *(vii)* Implantation of an NGC to close a 15-mm sciatic nerve defect in rats. Reprinted from Ref. [31] with permission from Elsevier. (B) Preparation of a piezoelectric conductive core–shell conduit. *(i)* Electrospinning. *(ii)* Rolling of the electrospun scaffold. *(iii)* Crosslinking of the conduit. *(iv)* Closing the bottom of the conduit with aluminum foil and injection of hydrogel into it. *(v)* Freeze-drying. *(vi)* Opening the top and bottom of the conduit. Reprinted from Ref. [12] with permission from Taylor & Francis. (C) A multichannel electroactive NGC *(iii)* composed of an SF/PEDOT cryogel scaffold *(i)* and PVDF/poly (L-lactic acid--*co*-caprolactone) [PLCL] film *(ii)*. Reprinted from Ref. [11] with permission from Elsevier.

mechanical interaction between cells and the network. Two distinct stages of cell adhesion were distinguished (Fig. 7A), including (i) slippage and (ii) traction. The system generated piezopotential only when cell differentiation was needed, without the piezopotential during cell spreading and adhesion. *In vitro* assays of rBMSCs on the PVDF scaffolds showed their ability to support cell survival, adhesion, and spreading (Fig. 7B). Moreover, there were more cells on a-PVDF than on r-PVDF or TCP, and cellular neurites on a-PVDF extended along the fiber direction much more than those on the r-PVDF scaffold (Fig. 7D–F). Expression levels of both neural and neurogliocyte makers in the cells on piezoelectric PVDF scaffolds were higher than those on TCP (Fig. 7C). These results indicate that piezoelectric PVDF scaffolds may specifically enhance neuron-like differentiation of rBMSCs, and a-PVDF is more advantageous.

Seeding of biosynthetic conduits with viable SCs is a well-established strategy to improve axonal regeneration after peripheral-nerve or spinal

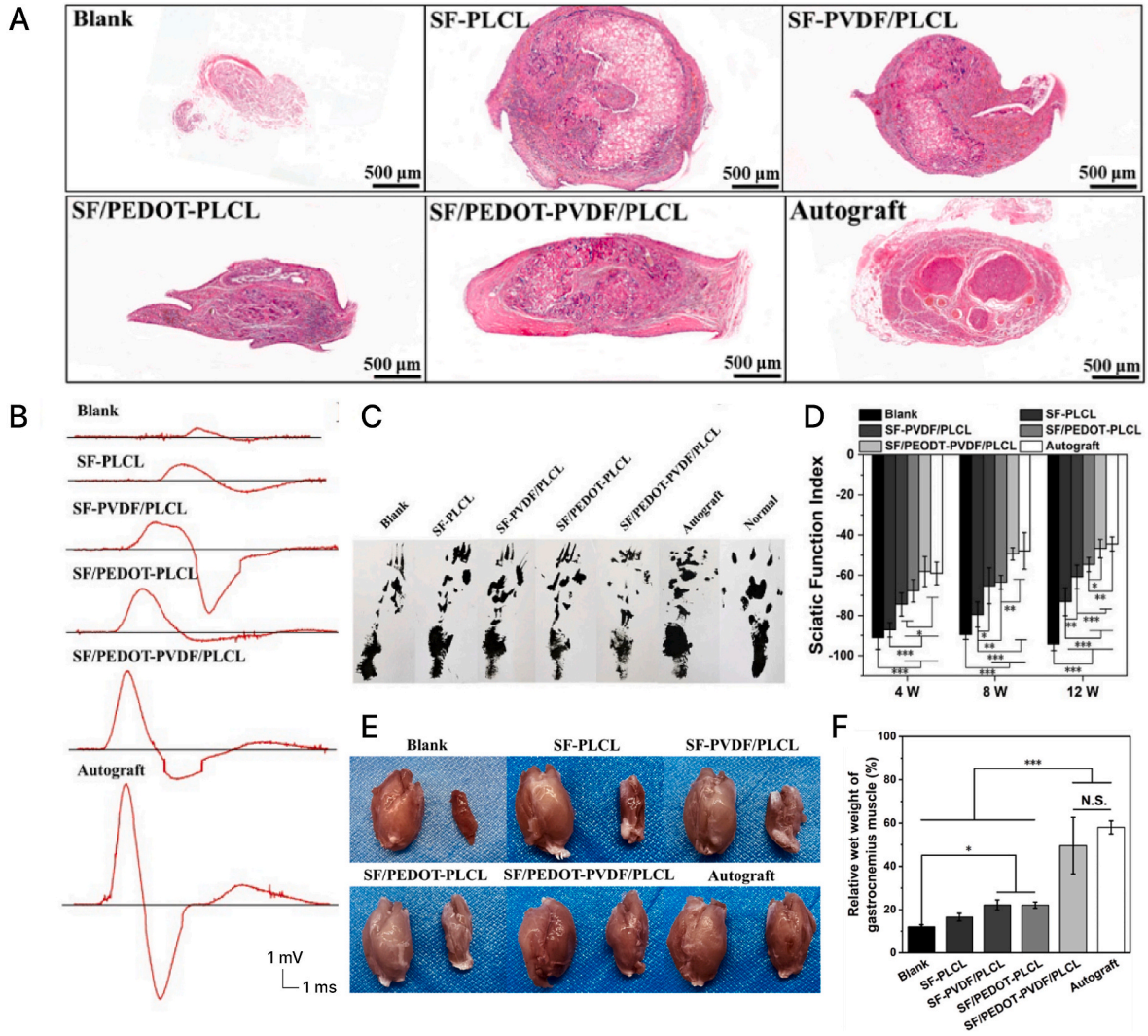

Fig. 10. *In vivo* evaluation of a piezoelectric conductive SF/PEDOT-PVDF/PLCL conduit. (A) Transverse sections of regenerated nerves. (B) CMAP recordings on the injured side of the rats. (C) Photographs of rat footprints after painting with black ink. (D) The SFI at 4, 8, and 12 weeks after the surgical operation (*$p < 0.05$, **$p < 0.01$, and ***$p < 0.001$). (E) Gross images of isolated bilateral gastrocnemius muscles in each group. (F) The gastrocnemius wet weight recovery ratio (injured side/contralateral normal side). Reprinted from Ref. [11] with permission from Elsevier.

cord injury [123]. SCs are responsible for the supportive environment within biosynthetic conduits because they produce ECM molecules, integrins, and neurotrophins [124]. Authors of ref. [101] were the first to utilize nanofibrous piezoelectric P(VDF-TrFE) conduits filled with SCs for spinal cord repair (for 3 weeks). *In vivo* assays (Fig. 8) suggested that both conduits supported (i) SC survival, (ii) regeneration of sensory ($CGRP^+$) and brainstem ($D\beta H^+$) axons across the spinal cord/conduit interface, (iii) extension of astrocyte/$GFAP^+$ processes into the conduit, and (iv) blood vessel formation. Aligned fibrous conduits contained a significantly greater number of $GFAP^+$ processes (Fig. 8A, *$P < 0.05$) and of $D\beta H^+$ axons (Fig. 8B, *$P < 0.05$) than did randomly aligned fibrous conduits. Notably, SCs and NF^+ axons extended along the conduit, parallel to the rostral–caudal axis, corresponding to the direction of the aligned fibers (Fig. 8G).

The high piezoelectricity, flexibility, and biocompatibility of PVDF and P(VDF-TrFE) make them good candidates for use in tissue engineering [12,28,31,33,47,48,97,99,101,103]. As one can see in Table 2, PVDF and P(VDF-TrFE) scaffolds have shown good potential for promoting the adhesion, survival, proliferation, neural differentiation, and other useful characteristics of various cells, including SCs, DRG neurons, NSCs, PC12 cells, rBMSCs, and other cell types *in vitro*. Meanwhile *in vivo* assays of conduits based on these polymers are still addressed in very few papers [69,100,101]. Most of the current research is focused on *in vitro* assays with piezoelectric nerve scaffolds, which are only experimental samples rather than ready-for-use medical devices. In the future research, attention should be given to the performance of tubular piezopolymer conduits *in vivo*, especially in long-distance nerve defect models over 2 cm.

A number of techniques have been utilized to obtain PVDF-based scaffolds, including solvent casting, heat-melt extrusion, and electrospinning. Among these techniques, the electrospinning of aligned fibrous scaffolds and NGCs stand out as an ideal approach due to its ability to mimic characteristics of the native neural ECM, exceptional porosity, facilitated transport of nutrients and oxygen to cells, and the ease of functionalization with bioactive molecules and viable cells. By contrast, only insufficient nerve regeneration can be achieved by the rigid melt-extruded P(VDF-TrFE) conduits due to the lack of permeability [100].

There are several drawbacks associated with the use of neat PVDF-based conduits in neural tissue engineering, including the lack of biodegradability and of biological activity, unacceptable hydrophobicity, and excessive stiffness. PVDF-based composites can make up for the shortcomings of the single material and maximize PVDF performance. Therefore, composite scaffold materials have become the focus of

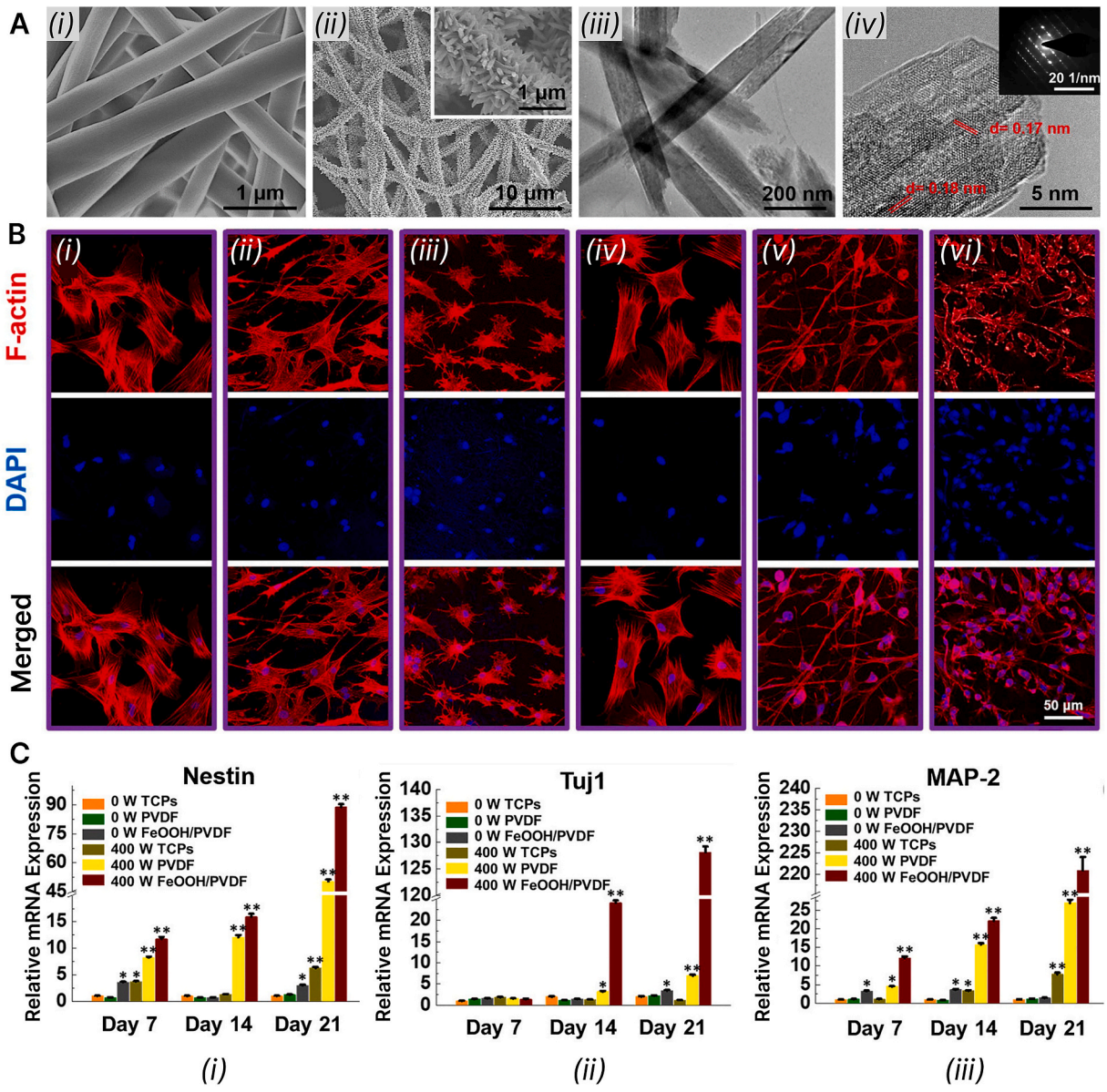

Fig. 11. Ultrasound-driven electrical stimulation of rBMSCs' neural differentiation on a piezoelectric nanofibrous hybrid membrane. (A) SEM images of pure PVDF *(i)* and FeOOH/PVDF *(ii)* membranes. Transmission electron microscopy *(iii)* and high-resolution transmission electron microscopy *(iv)* images of FeOOH nanorods. (B) rBMSC morphology on different substrate samples after 21 days of culturing with or without ultrasonication: *(i)* TCP, 0 W. *(ii)* PVDF, 0 W. *(iii)* FeOOH/PVDF, 0 W. *(iv)* TCP, 400 W. *(v)* PVDF, 400 W. *(vi)* FeOOH/PVDF, 400 W. F-actin was stained red by rhodamine phalloidin, and cell nuclei were stained blue by DAPI. (C) Neural differentiation of rBMSCs cultured on different substrate samples with or without ultrasonication. Quantitative-PCR analysis of the expression of neural-cell–specific genes: *(i)* nestin, *(ii) Tuj1*, and *(iii) MAP2* in the cells cultured on the different substrate samples at 7, 14, and 21 days. All data represent means ± SD (n = 3). *0.01 < p < 0.05; **p < 0.01. Reprinted from Ref. [99] with permission from Elsevier.

current tissue engineering research.

5.1.1. *PVDF-based hybrids*

Development of smart composite PVDF- and P(VDF-TrFE)-based materials (Table 3) can help to achieve the desired properties required for neural tissue engineering scaffolds, e.g., biodegradability, improved mechanical characteristics, an enhanced piezoresponse, and conductivity [11,12,97,99]. Fig. 9 exemplifies the multistage techniques for preparation of composite PVDF-based conduits. It has been found that the addition of 80 wt% of PCL to PVDF simultaneously improves biodegradation, mechanical properties, and biocompatibility of neat PVDF [31]. At 4 months after implantation into 15-mm rat sciatic nerve defects, the PVDF/PCL conduits (Fig. 9A) had an SFI of −27.7 %, which was significantly higher than that of the PCL group (−41.5 %).

Piezoelectric capacity of PVDF-based scaffolds can be improved by the addition of nanofillers, such as silica nanoparticles, ZnO, graphene-based materials, and piezoceramics [12,28,68,97,125]. The electrical stimulation can be further boosted by supplementation with electroconductive materials, for example, polyaniline/graphene (PAG) nanocomposites or poly-PEDOT [11,12,97]. Mohseni et al. [97] have constructed self-powered conductive scaffolds by chopping electrospun PVDF nanofibers doped with mesoporous silica nanoparticles (PVDF/MCM41) followed by incorporation into gellan/PAG nanocomposites. The addition of up to 15 wt% of MCM41 resulted in an enhanced output voltage of ~230 mV. This phenomenon was ascribed to a sufficient effective interaction between PVDF CH_2 groups and MCM41 nanoparticles; this interaction possibly increased charge voids and electrical dipoles as compared to neat PVDF. Meanwhile, incorporation of up to 2 wt% of PAG led to higher scaffolds' conductivity, up to 12×10^{-5} S/cm. Finally, the scaffolds promoted PC12 cell growth, with

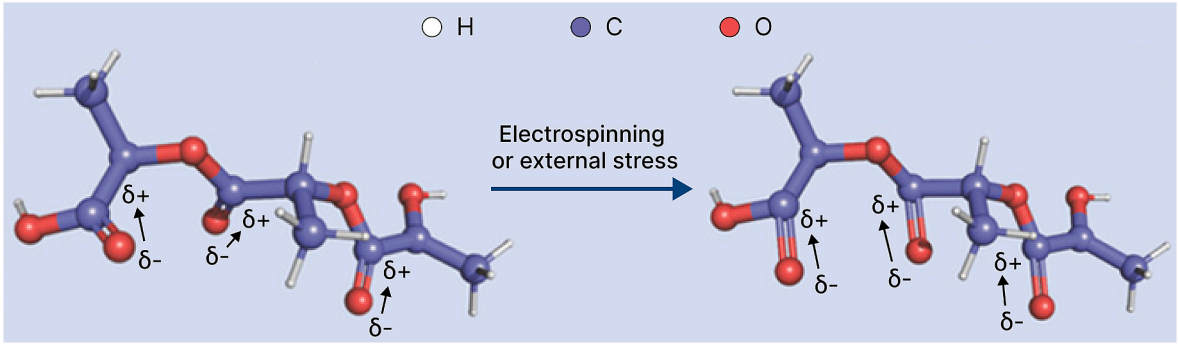

Fig. 12. Molecular structure of a PLLA chain with orientation of C=O dipoles in all directions or preferential orientation of the C=O dipoles after electrospinning. Adapted from Ref. [36] with permission from Wiley.

physicochemical parameters acceptable for neural cells [97].

Javidi et al. [12] have designed a core–shell conduit with conductive, antibacterial, and highly piezoelectric properties by a multistep process (Fig. 9B). First, shell structure was fabricated by the rolling of coelectrospun mats of PCL/PVDF and gelatin impregnated with PAG nanocomposites (Fig. 9B, *i, ii*). Then, the fabricated conduits were filled with gelatin/chitosan hydrogels containing PAG and ZnO nanoparticles (Fig. 9B, *iv*). Output voltage was enhanced up to approximately 1000 mV due to a synergistic effect of ZnO and PAG. Moreover, the addition of PAG to the conduit increased the conductivity from virtually an insulator's conductivity to 8.9×10^{-5} S/cm. The co-spun PCL/PVDF/gelatin shell impregnated with 2 wt% of PAG promoted proliferation of PC12 cells. Filling the conduit with hydrogels containing PAG and ZnO further boosted cell viability and proliferation, and this effect was attributed to the hydrophilic nature of chitosan/gelatin hydrogels.

To enhance polymer/filler interface bonding for efficient improvement of piezoelectric properties, surface modification can be carried out, for example, by *in situ* dopamine polymerization [28,126]. Chen et al. [28] have devised ultrasound-driven piezoelectric thin-film nanogenerators by electrospraying PVDF with polydopamine (PDA)-coated $0.5Ba(Zr_{0.2}Ti_{0.8})O_3$-$0.5(Ba_{0.7}Ca_{0.3})TiO_3$ (BZT-BCT@PDA) nanowires. Incorporation of up to 50 wt% of BZT-BCT@PDA into the PVDF thin films enhanced their output voltage from 2.5 to 13.5 V. Remnant polarization and the d_{33} coefficient of the composite thin films also went up as the mass proportion of BZT-BCT@PDA nanowires increased. Direct electrical neurostimulation was successfully achieved in a rat model of sciatic nerve injury [28].

As stated above, besides sufficient piezoelectric capacity, an NGC should be able to maintain electrical-signal conduction. Ma et al. [11] have fabricated a conductive NGC by PEDOT *in situ* polymerization on a porous SF cryogel (Fig. 9C, *i*). Then, a piezoelectric biodegradable PVDF/PLCL film was cast (Fig. 9C, *ii*) and wrapped in the outer layer of the SF/PEDOT cryogel (Fig. 9C, *iii*). *In vivo* results (Fig. 10) showed that the electroactive NGC significantly promotes peripheral nerve regeneration and functional recovery after 12 weeks in the rat model of sciatic nerve injury, by achieving the repair effect of autografts through synergistic effects of piezoelectric and conductive properties of the NGC.

Ferrous particles are promising fillers for nerve scaffolds because iron ions have been found to positively affect neural differentiation [99,127,128]. Zhang et al. [99] have constructed FeOOH/PVDF nanofibrous hybrid membranes by hydrothermal assembly of a layer of FeOOH nanorods on PVDF membranes (Fig. 11A) to investigate the synergetic effect of piezoelectricity and an iron ion release on neural differentiation of stem cells. During ultrasonication, piezoelectric potential and the electrically driven iron ion (Fe^{3+}) release could not only modulate rBMSC attachment, spreading, proliferation, and migration (Fig. 11B) but also accelerated the neural differentiation of rBMSCs (Fig. 11C). Gene and protein expression assays suggested that typical neural-cell–specific genes (nestin, *Tuj1*, and *MAP2*) of the cells cultured on FeOOH/PVDF membranes were significantly upregulated (89-, 128-, and 220-fold, respectively) after ultrasonication as compared to cells on TCP during the same treatment (Fig. 11C).

Table 3 indicates that hybrid PVDF-based NGCs have achieved good results in practical applications owing to the complementary characteristics of each individual material. Composites made of multiple polymers can make up for the shortcomings of a single polymer and combine their advantages to improve overall performance. For instance, introduction of biodegradable polymers, including PCL, gelatin, or chitosan, not only enables the resorption of PVDF-based composite scaffolds under physiological conditions but also can improve the hydrophilicity, biocompatibility, and mechanical characteristics of these materials [11,12,31]. Nevertheless, nonpiezoelectric polymers can obviously reduce the piezoelectricity of the composite scaffold to some extent [31]; hence it is important to optimize the composition to strike a balance between required degradability and sufficient piezoelectric capacity. In this regard, the addition of nanofillers, such as silica nanoparticles, ZnO, graphene-based materials, and piezoceramics, can greatly influence piezoelectric performance of PVDF-based nerve scaffolds [12,28,68,97] and thereby improve their nerve regeneration abilities. Finally, magnetic particles have been incorporated into piezoelectric devices to ensure their mobility [98,129].

5.2. PLLA-based scaffolds

In vivo applications of common biocompatible piezoelectric PVDF and P(VDF-TrFE) materials necessitate an invasive surgical procedure for removal of the implant. In this regard, PLLA is a promising candidate for tissue engineering scaffolds owing to its biodegradability [88]. PLLA is a biodegradable biocompatible polymer with a high shear piezoelectric coefficient (d_{14}) of approximately −10 pC/N [10]. PLLA is degraded by hydrolytic degradation, and a byproduct (PLA) is nontoxic and water-soluble. Fig. 12 (left) presents PLLA in the thermodynamically stable α-crystalline phase, where C=O dipoles are helically oriented along the main backbone chain [130,131]. To induce piezoelectricity, the chains must be thermally stretched to transform the α-phase into β-phase, which represents a change from randomly oriented molecular chains to molecular chains aligned along the stretch direction [131]. The electrospinning process can also align the C=O bonds to create piezoelectric PLLA as shown in Fig. 12 (right).

Just as other synthetic polyesters, PLLA has a hydrophobic nature, which may negatively affect cellular adhesion [88,90], and surface modification is a promising solution. To address the hydrophobicity, Xia et al. [88] have performed a robust modification of PLLA nanofibers by electrostatic interaction with dopamine and its *in situ* polymerization (Fig. 13). PDA modulation was achieved with the help of ultrasound, which was employed to activate a piezoelectric nanofiber to create surface charges (Fig. 13A). The WCA of the PDA-modified PLLA scaffolds shifted from 117° to 0° (Fig. 13B, *i, ii*), giving surface wettability

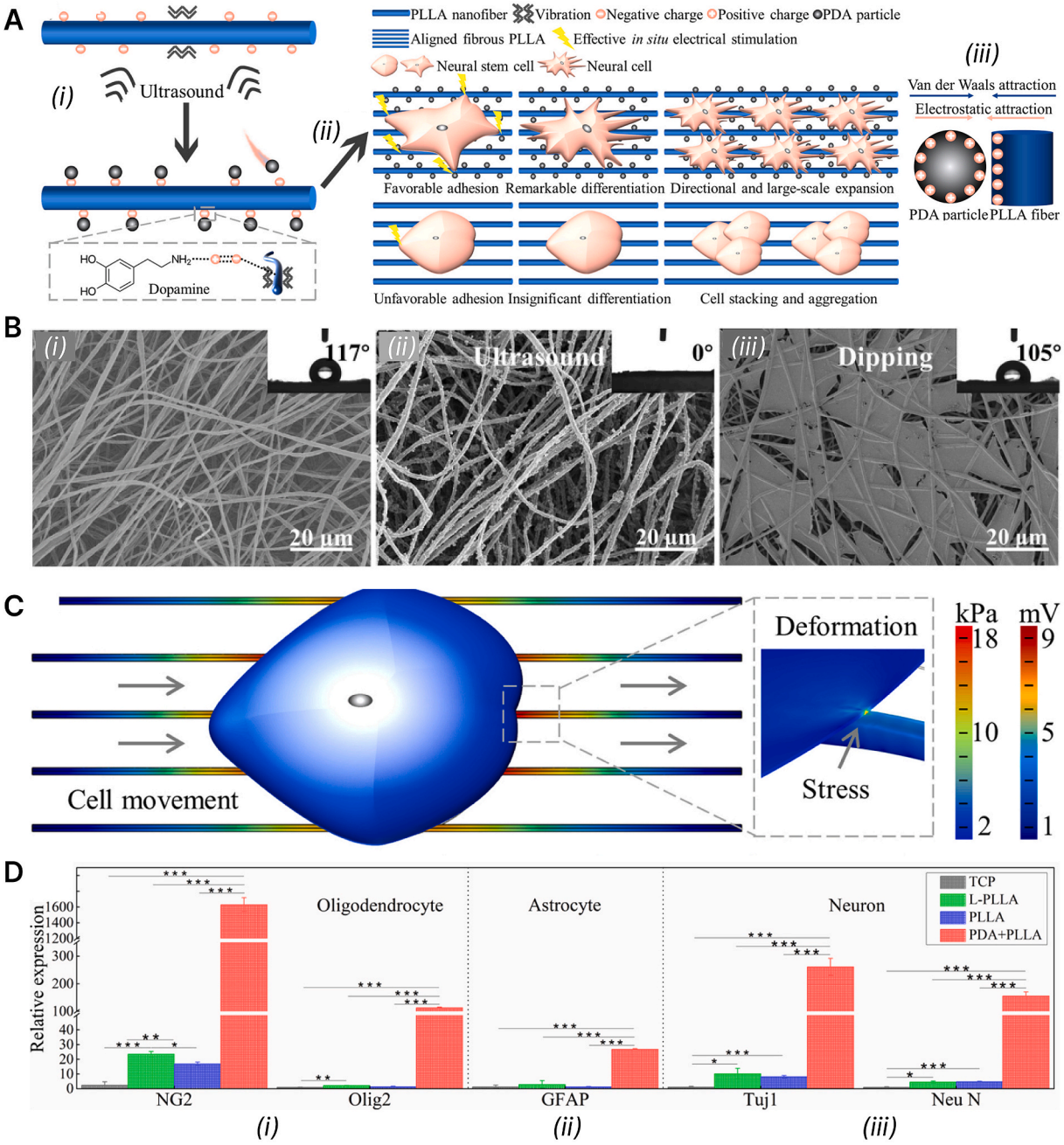

Fig. 13. Electrostimulation of stem cell differentiation on hydrophilic PLLA nanofibrous scaffolds. (A) PDA modification of PLLA nanofibers under ultrasonication and application of this modification for NSC differentiation and expansion. *(i)* Piezoelectric charges inducing dopamine *in situ* polymerization on a PLLA nanofiber. *(ii)* The PDA-modulated scaffold provides favorable adhesion conditions and transmits electrical cues and oriented topography signals. *(iii)* Proposed interaction between PDA and PLLA fibers. (B) SEM images of *(i)* fibrous PLLA, *(ii)* fibrous PLLA with PDA modified via ultrasonication, and *(iii)* fibrous PLLA with PDA modified via dipping. The inset refers to the corresponding contact angle. (C) Electric potential and stress of oriented piezoelectric nanofibers under the influence of cell movement. (D) Quantitative-PCR analysis of the expression of neural-cell–specific genes: *(i)* oligodendroglia-related genes (*NG2* and *Olig2*), *(ii)* an astrocyte-related gene (*GFAP*), and *(iii)* neuron-related genes (*Tuj1* and *NeuN*). Asterisks denote statistically significant differences: *$p < 0.05$, **$p < 0.01$, and ***$p < 0.001$. Reprinted from Ref. [88] with permission from Elsevier.

satisfactory for cell adhesion. Moreover, the attached PDA particles enhanced surface roughness, offering more cell adhesion sites. Seeding of NSCs on the piezoelectric PLLA-PDA scaffolds showed significant cell proliferation and differentiation into nerve cells on day 7 without exogenous growth factors (Fig. 13D).

Graphene-based materials have emerged as ideal electroactive fillers for nerve scaffolds with high electrical conductivity and low cytotoxicity [8,29,132]. Yang et al. [29] have fabricated a self-powered electroconductive NGC by incorporation of carbon nanotubes (CNTs) into GelMA with subsequent embedding of the CNTs@GelMA composite hydrogel into an aligned electrospun PLLA piezoelectric conduit (Fig. 14A). Weak electricity (on the PLLA nanofibers' surface) generated by body movements was transferred to nerve fibers and SCs through the conductive CNTs@GelMA hydrogel, which could change cell membrane potential and increase cell excitability. The scaffold was applied to a 10-mm rat sciatic nerve defect for 12 weeks, which significantly facilitated peripheral nerve regeneration and enhanced motor functional recovery as evidenced by the improved SFI, CMAP, and muscle weights

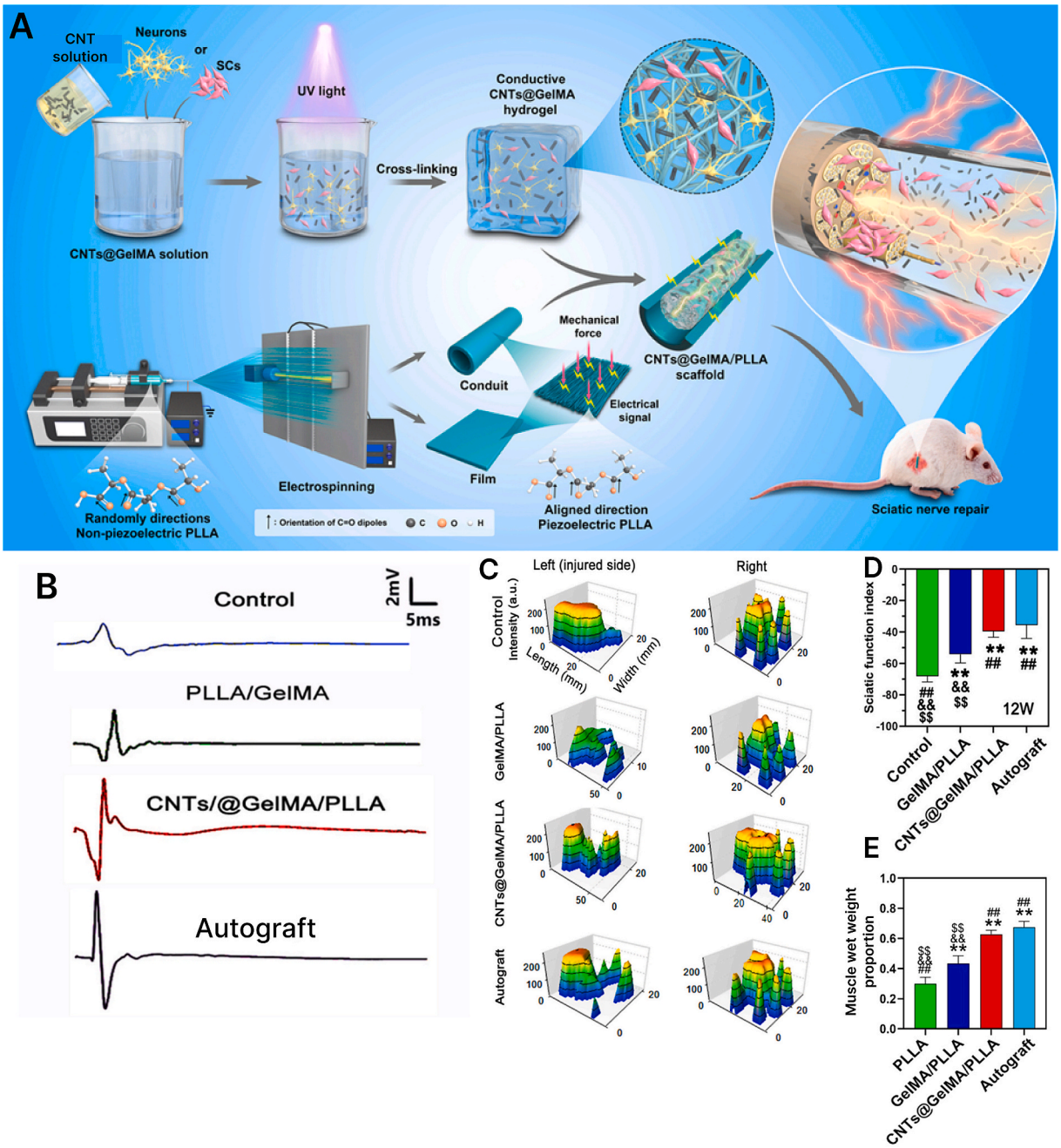

Fig. 14. An electroconductive composite scaffold promotes peripheral nerve regeneration. (A) Schematic illustration of the manufacturing process and biomimetic application of a wirelessly self-powered electroconductive CNTs@GelMA/PLLA device. Functional recovery of transected sciatic nerves. (B) Latency and amplitude of CMAP in control, GelMA/PLLA, CNTs@GelMA/PLLA, and autograft groups at 12 weeks postoperation. (C) Footprint images of control, GelMA/PLLA, CNTs@GelMA/PLLA, and autograft groups at 12 weeks. (D) The SFI in different groups at 12 weeks. (E) Weight percentages of muscle fiber areas in four groups. All statistical data are presented as mean ± SD (n = 3); *$p < 0.05$ for a comparison with the control group; **$p < 0.01$ for a comparison with the control group; $^{\#\#}p < 0.01$ for a comparison with the GelMA/PLLA group; $^{\&}p < 0.05$ for a comparison with the CNTs@GelMA/PLLA group; $^{\&\&}p < 0.01$ for a comparison with the CNTs@GelMA/PLLA group; $^{\$}p < 0.05$ for a comparison with the autograft group; $^{\$\$}p < 0.01$ for a comparison with the autograft group. Reprinted from Ref. [29] with permission from Elsevier.

(Fig. 14B–E).

Magnetic nanofillers are often introduced into scaffolds to actuate their mobility [98,129] for high-precision minimally invasive therapies. Magnetic scaffolds can be manipulated with a magnetic field *in situ* to provide directional guidance to neurons. Magnetic materials can also transport cells to target areas, and this property is crucial for targeted cell therapy of neural diseases. Chen et al. [98] have developed multifunctional soft microrobots of helical bodies consisting of a PLLA piezoelectric matrix impregnated with CFO magnetic nanoparticles (Fig. 15A, *i–ii*). With the application of a rotating magnetic field, the microrobots could swim in a corkscrew fashion in different body fluids. When subjected to ultrasound waves, the piezopolymer matrix could electrically polarize and thereby induce the differentiation of PC12 cells loaded on the swimmers' surface (Fig. 15A, *iii*). In turn, Johnson et al. [129] have electrospun aligned superparamagnetic iron oxide nanoparticle (SPION)-loaded PLLA microfibers (Fig. 15B, *i, ii*), which were injected into collagen or fibrinogen hydrogels (Fig. 15B, *iii*) and repositioned using an external magnetic field (Fig. 15B, *iv*) to implement

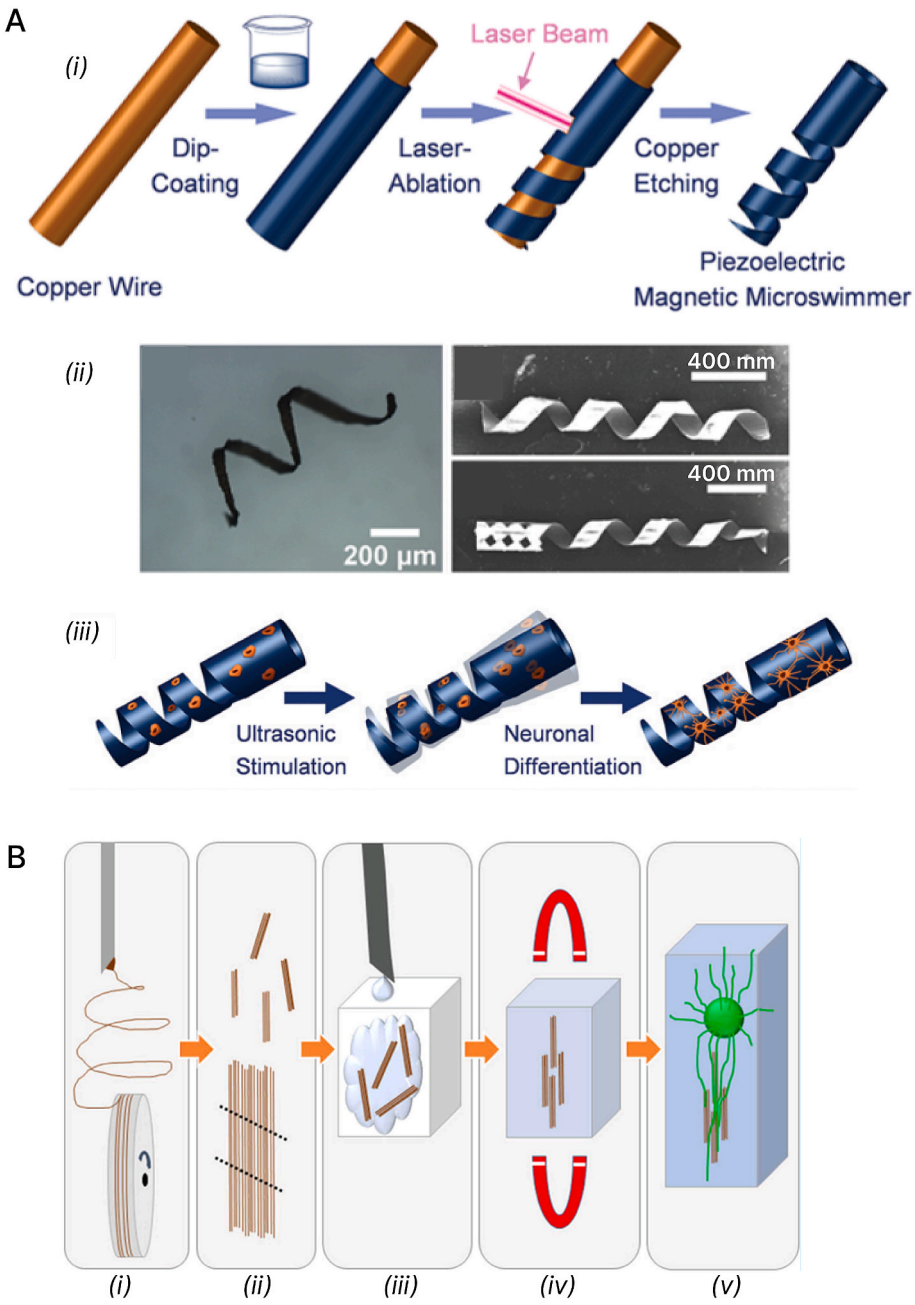

Fig. 15. Magnetic devices for nerve regeneration applications. (A): *(i)* Fabrication of piezoelectric magnetic microswimmers from PLLA/CFO. *(ii)* Optical (left) and SEM (right) images of helical microswimmers. *(iii)* Ultrasonic stimulation of the piezoelectric microswimmers induces neuronal differentiation of PC12 cells. Reprinted from Ref. [98] with permission from RSC. (B) Preparation of a PLLA/SPION composite scaffold. *(i)* Electrospinning of a PLLA/SPION aligned-fiber mat. *(ii)* Cutting the mat and rolling it into a small conduit that fits through the inner bore of the needle. *(iii)* Injection of the conduits and the hydrogel into a chamber. *(iv)* Orienting of the fibers within the hydrogel through the use of a magnetic field *in situ*. *(v)* Guiding of neurites extending from the DRG in a hydrogel injected with PLLA/SPION conduits. Reprinted from Ref. [133] with permission from Elsevier.

minimally invasive delivery of topographical guidance cues to DRG neurons (Fig. 15B, *v*). As a result, neurites growing from DRG explants extended 1.4 to 3 times farther on the aligned PLLA fibers as compared with the pristine hydrogel. In addition, magnetic scaffolds can apply tension to organelles and to the plasma membrane, thus stimulating tissue regeneration in an external magnetic field. For instance, culturing of DRG cells on SPION-grafted aligned PLLA fibers in an alternating magnetic field induces a 30 % increase in neurite length and a 62 % increase in neurite area as compared to DRG cells cultured on PLLA fibers with untethered SPIONs added to the culture medium [133].

Overall, PLLA has been shown to be a promising material for fabrication of both neat and composite nerve grafts (Table 4) owing to its biocompatibility, biodegradability, sufficient piezoelectricity, spinnability, and ease of hydrophilizing. Concerning the latter, modification of PLLA scaffolds with PDA [88] results in the superhydrophilicity of the modified PLLA, which is undesirable for efficient cell attachment [87]. Moreover, the degradation rate of the modified scaffolds can accelerate due to the increased hydrophilicity, which can actuate premature impairment of the scaffolds' mechanical and piezoelectric performance. Accordingly, it is worthwhile to find a golden mean between scaffolds' moderate hydrophilicity and prolonged integrity and electroactivity. Moreover, it is well known that PLLA piezoelectric capacity is poorer than that of PVDF or P(VDF-TrFE). In this regard, PLLA electroactivity can be enhanced by nanofillers [126], and one should take into account

Table 4
A summary of PLLA-based devices for neural tissue engineering.

Scaffold (conduit) composition	Scaffold fabrication and characterization	Piezoelectric performance	Biological model	Key outcomes	Ref.
In vitro					
PLLA	Electrospinning of aligned fibers with diameters from 30 to 500 nm; annealing	Effects of the fiber diameter and heat treatment temperature were demonstrated	human NSC differentiation	PLLA nanofibers enhanced neurogenesis by orthogonal piezoelectricity	[30]
PLLA	Electrospinning of PLLA fibers with a diameter of 500–700 nm. The scaffolds' WCAs before and after plasma treatment were 110.65° and 46.25°, respectively	A local effective piezoelectric signal was 4.2 mV. Output voltage was 0.5 V under 300 W ultrasonication	NSC proliferation	PLLA under ultrasound vibrations enhanced expansion of NSCs without growth factors. A stimulatory effect of PLLA on NSCs' proliferation rather than on neural differentiation was shown	[90]
PLLA	Electrospinning of aligned fibers with a diameter of 2 μm	Not reported	DRG neurons	The combination of topographical and electrical cues resulted in a 126 % increase in neurite outgrowth relative to unstimulated film controls	[94]
PLLA-PDA	*In situ* polymerization of dopamine on PLLA electrospun nanofibers. Modification with PDA changed the scaffold WCA from 117° to 0°. PDA particles increased surface roughness from 5 to 30 nm. A PLLA-PDA scaffold showed an accelerated biodegradation rate as compared to pure PLLA	1.76 mV (upon a deformation of 96 nm)	NSC differentiation	Cells expanded and differentiated into nerve cells on day 7 without exogenous growth factors. The topography of oriented nanofibers induced directional growth of the cells along aligned nanofibers	[88]
PLLA-SPIONs (up to 8 wt%)	Electrospinning of aligned fibers with a diameter of ~2 μm. The magnetization of the fibers was up to 4 emu/g. The fibers were injected into a collagen hydrogel and oriented in an external magnetic field	Not reported	DRG explants	SPIONs increased neurite outgrowth by 30 %. Neurites extended up to 3 times farther on the aligned PLLA fibers as compared with the pristine hydrogel	[129]
PLLA-SPIONs	Electrospinning of aligned fibers with a diameter of 2.2 ± 0.3 μm followed by SPION grafting onto the fibers' surface. The WCA of the scaffold was 123.8 ± 8.5°. The average grafting density was 39 ± 18 SPIONs/μm^2	Not reported	DRG explants	The alternating magnetic field increased neurite length by 40 % on control fibers as compared to a static magnetic field. Stimulation with an alternating magnetic field yielded a 30 % increase in neurite length and a 62 % enlargement of neurite area on SPION-grafted fibers compared to a DRG cultured on PLLA fibers with untethered SPIONs added to the culture medium	[133]
In vivo					
CNTs@GelMA/PLLA	The CNTs@GelMA composite hydrogel was embedded into an aligned electrospun nanofibrous PLLA conduit. The double-layer NGC had a mechanical strength of 10 kPa	Surface potential of the PLLA film was 7.3 mV. Output voltage of CNTs@GelMA/PLLA was 5.96 V	SCs; DRGs; 10-mm rat sciatic nerve defect (12 weeks)	Improved adhesion and elongation of SCs; promoted axonal outgrowth and elevated the neurite number in DRGs. Facilitated peripheral nerve regeneration: an enhanced motor functional recovery as revealed by the improved SFI (−39.6 ± 3.8) and muscle weights	[29]
PLLA/PHBV/KNN (50 wt%)	Potassium sodium niobate (KNN) nanowires with diameters of 300 nm were synthesized by a solid-state reaction. A PHBV/PLLA/KNN thin film was prepared by spin coating. Young's modulus of the PHBV/PLLA/KNN film was 44 N/mm^2	Output voltage and the output current were 6 V and 0.6 μA, respectively	Rat sciatic nerve injury (12 weeks)	Enhanced nerve regeneration proven by a function recovery analysis, histological assessment, and microstructure analysis. The SFI was −41.2 (similar to that of the autograft)	[126]

the degree of dispersion and interaction between the nanofiller and the polymer matrix. Another interesting alternative is composite scaffolds containing an electroconductive polymer, e.g., polyaniline or PEDOT, aside from a piezoelectric polymer. It has been demonstrated that the addition of an electroconductive phase to piezoelectric materials increases piezoelectricity [11,12,97,105].

In a rat model of sciatic nerve injury, an enhanced motor functional recovery of peripheral nerves has been achieved by various PLLA-based conduits with an SFI of approximately −40 (12 weeks postoperation) similar to that of the autograft [29,126]. Nonetheless, scientists believe that rodents are a poor model for the repair of human peripheral nerve defects because of differences from humans in the regeneration profile and neurobiology. Thus, more research is still necessary to design an optimized scaffold with high efficiency in clinical models, especially in the case of neural injuries with a gap size more than 30 mm.

5.3. PHA-based scaffolds

PHAs are promising materials for tissue engineering owing to their natural origin, a slow resorption rate with nontoxic byproducts [45,134–137], and mechanical stability [45,52,54,138]. Additionally, PHAs are known to possess neuroregenerative properties [52]. The relatively slow degradation rate of PHAs, as compared to commonly used PLLA, PGA polymers, or PLGA copolymers, is highly consistent with the slow regeneration of a nerve tissue [5,53,137]. Table 5 summarizes recent advances in PHA-based materials for neural tissue engineering. PHB is the most commercially available, well-studied, and commonly used member of the PHA family, widespread among prokaryotic cells (in the cytoplasm), especially bacteria. It has relatively low piezoelectric coefficient d_{14} of 1.3–2.0 pC/N [10,35]. Similarly to PLLA, the piezoelectricity of PHB is related to the presence of polar carbonyl groups in its multilamellar crystalline structure [34]. Unfortunately, PHB is intrinsically brittle and possesses mechanical properties inadequate for the

Table 5
A summary of PHA-based scaffolds and conduits for neural tissue engineering.

Scaffold (conduit) composition	Fabrication technique	Scaffold (conduit) characterization	Biological model	Key outcomes	Ref.
In vitro					
PHB vs. PHBV	Electrospinning vs. solvent-casting	Diameters of the PHB and PHBV fibers were 3.7 ± 1.7 and 2.3 ± 2.1 μm, respectively. PHBV fiber mats were more flexible than their PHB counterparts. Mechanical integrity of the cast films was much better than that of the fiber mats	SCs	Both types of materials were biocompatible; SCs proliferated on the smooth cast films better than on the rough fibrous scaffolds	[50]
PHB/PCL or P (3HB-co-4HB) shell; PHB core	Microextrusion and leaching (shell); melt spinning (core)	Shell thickness was 250–500 μm. The core fiber diameter was 20 μm. Optimal shell porosity and pore size were 55 % and 0.5 μm, respectively. Permeability of the shell for large molecules was demonstrated	DRG; sympathetic cervical ganglia (SCGs)	The NGCs supported neuron survival and neurite outgrowth. Introduction of fibrillar lumen fillers promoted oriented neurite growth, whereas coating with ECM proteins further increased ganglia attachment and cell migration	[5]
PHB/PHO at 25:75	Electrospinning	Aligned fibers of various diameters: 2.4 ± 0.3, 3.7 ± 0.3, and 13.5 ± 2.3 μm	NG108-15 neuronal cells	Facilitated cell growth, proliferation, and differentiation. The scaffold with a large fiber diameter (13.50 ± 2.33 μm) was the best for neurite outgrowth and differentiation	[52]
PHB/CTS 15 to 20 wt%	Electrospinning	Average fiber diameters in aligned scaffolds were 740–870 nm, i.e., less than those in randomly aligned fibrous mats. The addition of CTS (20 wt%) decreased WCAs from 111° to 33° for the aligned scaffolds. Tensile strength rose from 6.41 MPa in randomly aligned PHB/CTS 85:15 fibrous scaffolds to 8.73 MPa in the aligned ones. PHB/CTS lost 25 %–35 % of mass after 8-week degradation *in vitro*	B65 cells	Improved cell proliferation; bipolar neurite extensions and cell orientation in the direction of the fiber alignment	[45, 51]
PHB/PHBV/ collagen at 45:45:10	Electrospinning	Fiber diameter in aligned scaffolds was 963 ± 117 nm. The WCA of the PHB/PHBV/ collagen scaffold was 95° ± 9°	SCs	Improved adhesion, proliferation, and differentiation of SCs upon the collagen supplementation. Bipolar morphology of cells orienting along the fiber direction	[44]
Peptide-modified PHB/PHBV at 50:50	Electrospinning	Aligned fibers of 925 ± 156 nm. The WCA declined from 107.4° ± 5.0° for the untreated PHB/PHBV scaffold to 0° for the peptide-modified mat	SCs	A higher degree of spreading, metabolism, and proliferation of SCs on the functionalized scaffolds	[57]
PHBV/collagen at 50:50	Electrospinning	Aligned fibers of 229 ± 65 nm. Tensile strength, elongation, and Young's modulus of the aligned PHBV/collagen 50:50 scaffold were 6.3 ± 0.4 MPa, 13 % ± 3 %, and 193 ± 3 MPa, respectively	PC12 cells	40 % enhanced cell proliferation and facilitated differentiation due to the collagen addition	[55]
Collagen-cross-linked PHB	Electrospinning	Fiber diameters of 600 and 900 nm and WCAs of 135° and 52° were attained in the unmodified and collagen-cross-linked mats, respectively	SCs	Enhanced cell adhesion	[89]
In vivo					
PHBV/PLLA/ KNN@PDA nanowires	Spin coating	The KNN distribution in the PHBV/PLLA matrix improved due to the PDA modification. Remnant polarization and Young's modulus of the PHBV/PLLA/ KNN@PDA (50 %) film were 70 kV mm^{-1} and 44 N/mm^2, respectively	Rat sciatic nerve defect (12 weeks)	Significantly promoted controllable nerve repair	[126]
PHBHHx, PHBVHHx, or PLLA coated with fusion proteins	Solvent-casting	Interconnected porous structures with a grainy surface. The WCA of the PHBVHHx film decreased from ~100° to ~75° after coating with proteins	Rat NSCs	PHBVHHx coated with PhaP–Ile-Lys-Val-ala-Val (IKVAV) yielded the highest cell adhesion and proliferation, while the PLLA/ PhaP–IKVAV film gave better neural differentiation and neurite outgrowth	[54]
PHBHHx	Particle leaching	Maximal stress was 2.3 and 0.94 MPa for the conduits with nonuniform and uniform porosity, respectively. PHBHHx lost 20–24 % of mass after 3 months *in vivo*	10-mm rat sciatic nerve defect (1 month)	Rapid functional recovery of nerves, as evidenced by CMAPs in PHBHHx conduits	[53]
PHB modified with ECM molecules and SCs	Not described	Unidirectional fiber orientation	Rat cervical spinal cord injury	Facilitated attachment and proliferation of SCs; improved cell survival after the addition ECM molecules (i.e., fibronectin, laminin, and collagen); marked axonal regeneration within the graft	[123]
ASC-filled PHBV	Electrospinning	Aligned fibers of 635 nm	10-mm rat sciatic nerve defect (10 weeks)	Improved ASCs' adhesion, survival, and proliferation on aligned fibrous mats compared with randomly oriented ones. Better nerve regeneration, neurogenesis, and motor function recovery, with an SFI of −34.7 ± 1.2	[56]

(*continued on next page*)

Table 5 (*continued*)

Scaffold (conduit) composition	Fabrication technique	Scaffold (conduit) characterization	Biological model	Key outcomes	Ref.
PHB/CTS loaded with human MSCs	Electrospinning	Aligned fibers of 600 nm. Tensile strength, elongation at break, and Young's modulus were 3.8 ± 0.3 MPa, 4.2 % ± 0.7 %, and 116 ± 11 MPa, respectively	10-mm rat sciatic nerve defect (8 weeks)	Regenerative capacity of the PHB/CTS–hMSC conduits was superior to that of PHB/CTS but not as good as that of the autograft	[16]
PHB	The conduits were formed from PHB sheets	The fibers' orientation was along the conduit longitudinal axis. The conduit internal diameter was 1.6 mm	10-mm rat sciatic nerve defect (1 month)	Good axonal regeneration with negligible inflammatory-cell infiltration. Good angiogenesis at nerve terminals and through the walls of the conduit	[139]
PHB filled with alginate, fibronectin, and SCs	Commercial PHB conduits were loaded with an alginate matrix with addition of fibronectin and SCs	Not conducted	10-mm rat sciatic nerve defect (6 weeks)	Enhance nerve regeneration upon the addition of fibronectin and SCs to the conduits	[140]
PHB	The conduits were rolled from PHB sheets	Unidirectional fiber orientation along their long axes	2–4-cm rabbit peroneal nerve gap (63 days)	Completely bridged nerve gaps by day 42. Greater area of nerve fibers in the PHB group than in the autograft group	[141]
PHB-GGF	NGCs were formed from PHB sheets	NGCs consisted of compressed PHB fibers of 2–20 μm, running in a parallel direction	2–4-cm rabbit peroneal nerve gap (120 days)	A greater number of SCs, regenerated axons, and myelinated nerve fibers in the PHB-GGF conduit than in the control (pristine PHB). The GGF supplementation reduced muscle mass loss and led to complete limb reinnervation by day 63	[138, 142]

CTS: chitosan, ASCs: adipose-tissue–derived stem cells.

requirements of NGC construction [44,50]. To overcome the brittleness, PHB is frequently blended with other polymers (e.g., PCL, PLLA, chitosan, or other PHAs) [5,45,51,52,126], or copolymers are used instead, such as P (3HB-*co*-4HB) [5], PHBHHx [53,54], or PHBV [44,50,55–57]. Hinüber et al. [5] have compared a PHB/PCL blend and the P (3HB-*co*-4HB) copolymer for possible application to neural tissue engineering and found that the introduction of PCL improves bending and tensile properties of PHB. As a result, PHB/PCL proved to be stabler than P (3HB-*co*-4HB) and therefore more suitable for long-term regenerative applications [5]. These conduits successfully supported neuron survival and neurite outgrowth in an *in vitro* model of axonal regeneration involving DRG and sympathetic cervical ganglia [5]. A PHBHHx copolymer has also been investigated for possible application to the repair of damaged nerves [53,54]. PHBHHx conduits caused rapid functional recovery of rat sciatic nerve defects at 1 month post-implantation as well as manifested an ability to prevent connective tissues from ingrowth penetration [53].

The widely used PHBV copolymer possesses properties similar to PHB's but has higher flexibility [44,50]. Blending of PHB with PHBV is reported to improve both tensile strength and elongation at break of PHB/PHBV scaffolds compared to neat PHB [44]. PHBV has piezoelectric coefficient d_{14} of 1.3 pC/N [95] and therefore can be utilized in electroactive devices for nerve regeneration. In this regard, Wu et al. [126] have introduced a nanogenerator for PNI repair based on (1) biodegradable piezoelectric materials: PHBV, PLLA, and KNN nanowires; (2) biodegradable encapsulation layers of PLA; and (3) biodegradable magnesium electrodes and molybdenum wires (Fig. 16a). The PHBV/PLLA/KNN composite films showed excellent piezoelectric properties with d_{33} values significantly higher than d_{33} of a PVDF control film. To excite the piezoelectric PHBV/PLLA/KNN nanogenerators, ultrasound was chosen as an exterior wireless energy source (Fig. 16b). The implantable PHBV/PLLA/KNN piezoelectric nanogenerator could deliver *in vivo* electrical stimuli to the biodegradable conductive nerve conduits without any transcutaneous leads. The electrical output was adjusted by programmable ultrasound pulses with different input power intensity and waveforms. The results of a neurologic function recovery assay, histological assessment, and microstructural analysis confirmed good enhancement of nerve regeneration by the ultrasound-driven nanogenerator in a sciatic nerve injury model.

The hydrophobicity of PHAs is a shortcoming limiting their biomedical applications; hence, it is not desirable to use them alone for the fabrication of tissue engineering scaffolds. Alloying of PHB with natural polymers has emerged as an efficient way to render PHB hydrophilic [44,45,51,55]. For example, the addition of chitosan (20 wt%) decreases WCAs of aligned PHB/chitosan scaffolds from 125° to 43° and causes a noticeable enhancement of the porosity of the fibrous scaffolds [45,51]. Inherent physicochemical properties of chitosan such as biocompatibility and biodegradability, good cell adhesion, hydrophilicity, and nontoxicity have prompted its use in neural tissue engineering [16,45,51].

PHAs are also often blended with collagen [44,55,89]. The latter is the major component of the native ECM and induces only a weak immune response. Furthermore, collagen is a natural piezoelectric material with a piezoelectric coefficient in the range 0.2–2.0 pC/N [41]. A positive effect of collagen on biological performance of PHA electrospun scaffolds has been reported [44,55,89].

The surface of PHA-based scaffolds can be modified with various biomolecules, such as peptides, proteins, or growth factors, to enhance both their hydrophilicity and bioactivity. For instance, higher degrees of spreading, metabolic activity, and proliferation of SCs are seen when PHB/PHBV nanofibers are functionalized with synthetic peptides as compared to an unmodified scaffold [57]. Similarly, the introduction of ECM molecules (e.g., fibronectin, laminin, and collagen) into the surface of PHB-based conduits may significantly improve SC survival and proliferation [123,143]. In turn, coating of PHBHHx and poly (3-hydroxybutyrate-*co*-3-hydroxyvalerate-*co*-3-hydroxyhexanoate) [PHBVHHx] films with fusion proteins can promote the adhesion, proliferation, and neural differentiation of rat NSCs [54]. Glial growth factor (GGF) is a trophic factor specific for SCs. A PHB conduit containing GGF can significantly increase the regeneration of long rabbit peroneal nerve gaps, thus leading to motor organ reinnervation [138,142]. On post-operative day 120, GGF addition significantly elevated the number of SCs and mini-fascicles of myelinated fibers and reduced the muscle mass loss relative to controls [138,142].

Besides biofunctionalized scaffolds, nerve regeneration can be facilitated by scaffolds seeded with viable cells, such as SCs [48,101,123,140,144,145] or stem cells [16,56,146]. For example, aligned nanofibrous PHBV conduits loaded with neuronally differentiated MSCs facilitate the regeneration of 10-mm transected rat sciatic nerves as well as neurogenesis and recovery of motor function, with an SFI of −34.7 ± 1.2 (10 weeks postoperation) [56].

Many other studies point to positive outcomes of PHB-based NGCs in various *in vivo* models [140,139,141,147]. Among them, the rabbit peroneal nerve defect [138,142,141] is of great interest because to be

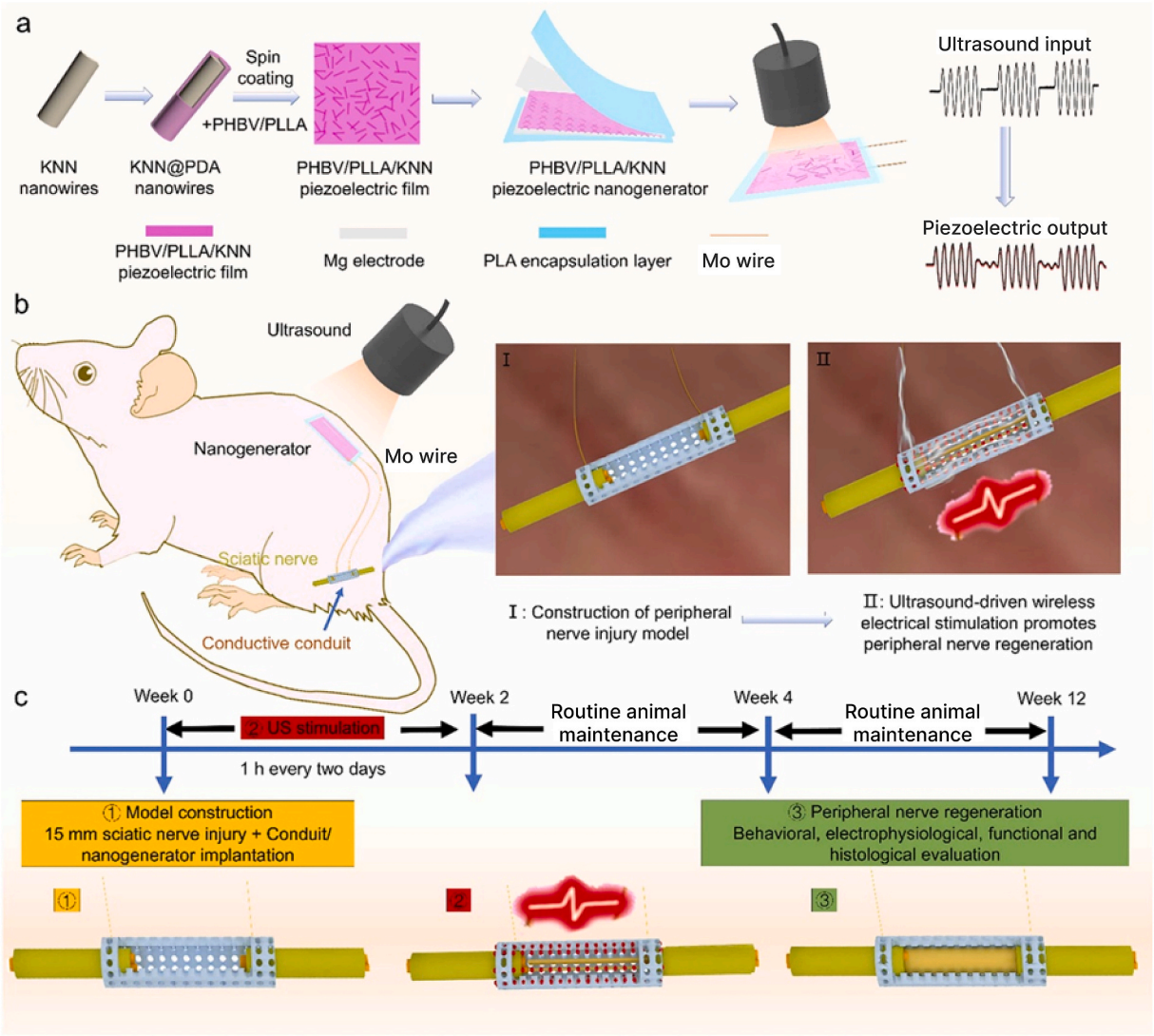

Fig. 16. Ultrasound-driven wireless electrical stimulation enhances peripheral nerve repair. (a) Fabrication of a PHBV/PLLA/KNN film nanogenerator; (b) the delivery of *in vivo* electrical stimulation by the implantable PHBV/PLLA/KNN film nanogenerator combined with ultrasound to enhance the peripheral nerve repair; (c) the scheme of repairing damaged peripheral nerves by ultrasound-driven wireless electrical stimulation. Reprinted from Ref. [126] with permission from Elsevier.

accepted into clinical practice, conduits must support regeneration of large gaps of over 2 cm. Young et al. [141] have investigated the potential of PHB conduits to bridge nerve gaps (up to 4 cm) in a rabbit model of common peroneal nerve injury. On day 42 postimplantation, the area of regenerating nerve fibers was greater in the PHB group than in the nerve autograft group, indicating that PHB conduits were capable of long-gap PNI repair.

Thus, PHAs are gaining popularity in tissue engineering, particularly neural tissue engineering (Table 5), because of their piezoelectric features, biocompatibility, biodegradability, high stability, good processability, and nontoxicity [44,51,55–57,123,148]. The aforementioned articles have shown good potential of various strategies to render nerve PHA scaffolds bioactive, including polymer blending [5,45,51,52], addition of natural polymers [44,45,51,55], supplementation with growth factors [138,142], seeding SCs or MSCs onto PHA scaffolds [16,56,123,146], and surface biofunctionalization with ECM molecules [89,123,143,140], synthetic peptides [57], or synthetic proteins [54]. In addition, the crucial role of topographical cues of scaffolds having aligned fibers in neural cells' attachment, proliferation, and differentiation has been abundantly discussed [44,45,52,55,56]. Nonetheless, to the best of our knowledge, only one study [126] deals with PHAs, namely a PHBV copolymer, as an electroactive material. Therefore, the impact of natural piezoelectric properties of PHAs on nerve regeneration is not fully understood though it is exceptionally relevant for such electrosensitive tissues as nerves. This knowledge gap opens an unexplored field for further investigation.

6. The role of piezoelectricity and conduit morphology in nerve repair

In addition to piezoelectric capacity, attention should be paid to the morphology of NGCs. In terms of structure, NGC walls should be highly porous and permeable to enable facile transport of nutrients, metabolites, and gases from the inner lumen to the surrounding environment and vice versa. Porous structure can mimic the perineurium that surrounds nerve fibers and allows for transport of nutrients *in vivo* [47]. Conduit porosity of 52.5 % ± 1.2 % has been found to be optimal for enabling nutrient and waste exchange while maintaining structural integrity [47]. Hinüber et al. [5] have investigated the diffusion of large molecules (70 kDa) through a PHA-based conduit wall. Permeation of 50 % of the molecules took less than 10 h at a wall thickness of 250 μm, and this rate was sufficient for effective diffusion of essential nutrients and metabolites through the conduit wall [5].

It is still unclear whether microfibers or nanofibers of scaffolds are

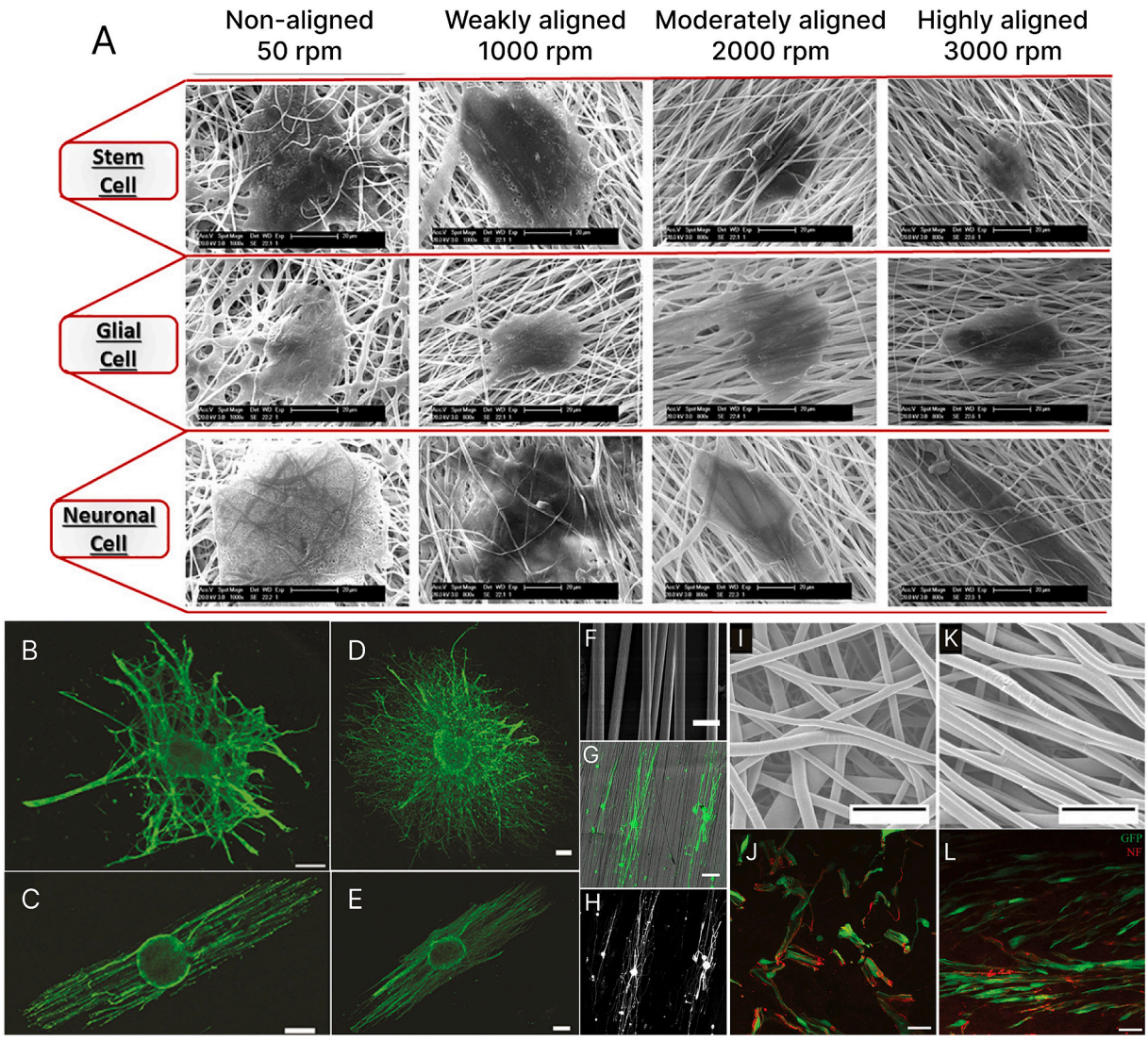

Fig. 17. Advantages of aligned fibers for neural tissue engineering. (A) SEM images of a stem cell, neuronal cell, and glial cell cultured on scaffolds with different fiber alignments. Reprinted from Ref. [70] with permission from Wiley. Confocal fluorescent images of a DRG stained with phalloidin (actin) on micron- (B–C) and nano-sized (D–E) randomly oriented (B, D) or aligned (C, E) P(VDF-TrFE) scaffolds (magnification: 4 ×, scale bar: 300 μm). Reprinted from Ref. [65] with permission from Wiley. (G–H) Primary rat neurons cultured for 12 h on laminin-coated PLLA fibers (F) with the addition of 4 wt% of Fe_3O_4. Reprinted from Ref. [129] with permission from ACS. SEM images of randomly oriented (I) or aligned (K) P(VDF-TrFE) fibrous scaffolds (scale bar: 5 μm); confocal fluorescence images of green fluorescent protein (GFP)-expressing SCs in the center of the graft in randomly aligned (J) or aligned (L) fibrous conduits. Scale bar: 50 μm. Reprinted from Ref. [101] with permission from Wiley.

better for neural tissue engineering applications. Positive results of nerve regeneration have been reported after the use of nanofibers [56,88,99,132,149–151] and microfibers [46,48,52,65,70,152–154]. Wang et al. have fabricated three groups of electrospun PLLA fibers (1325 ± 383 nm, microfibers; 759 ± 179 nm, submicrofibers; and 293 ± 65 nm, nanofibers) [153]. Nanofibers (293 ± 65 nm) did not promote extensive neurite extension or SCs' migration; submicron fibers (759 ± 179 nm) promoted long directed neurite extension independent of SC migration, whereas micro-scale fibers (1325 ± 383 nm) promoted both long directed neurite extension and SC migration [153]. In an *in vivo* study [151], nanofibrous NGCs yielded better results as compared to microfibrous NGCs in terms of the repair of 15-mm critical defect gaps. Nanofibrous conduits (251 ± 32 nm) yielded a significantly greater number of myelinated axons and thicker myelin sheaths as compared with microfibrous conduits (981 ± 83 nm). Lizarraga-Valderrama et al. [52] have generated electrospun PHA fibers with diameters of 2.4 ± 0.3, 3.7 ± 0.3, and 13.5 ± 2.3 μm and revealed a direct relation between fiber diameter and neuronal growth and differentiation. The greatest number of neuronal cells was seen on large fibers (13.5 ± 2.3 μm) when grown individually and in coculture with SCs. Thus, comparative studies on the fiber size effect in nerve regeneration remain contradictory and incomplete and require further investigation.

For an electrospun nerve scaffold, it is important to ensure a unidirectional alignment of fibers. Neuronal differentiation entails a number of specific events, including formation and extension of neuritic processes [155], and therefore it is crucial to create an aligned fibrous template for cells to extend and elongate on. Aligned topography is a versatile well-established simple strategy to improve nerve regeneration even without any additional biological and physicochemical stimuli [44,45,52,124,151,153,154,156–158]. After being implanted into a nerve injury site, the fibers that are aligned in the longitudinal direction of the conduit wall are able to guide regenerating axons to connect the stumps of the nerve defect. Moreover, longitudinally aligned structures can mimic myelinated axon white-matter tracts in the CNS [129]. Within a comprehensive project of Lins et al. [70], electrospun PVDF nerve scaffolds with various degrees of fiber alignment were prepared by

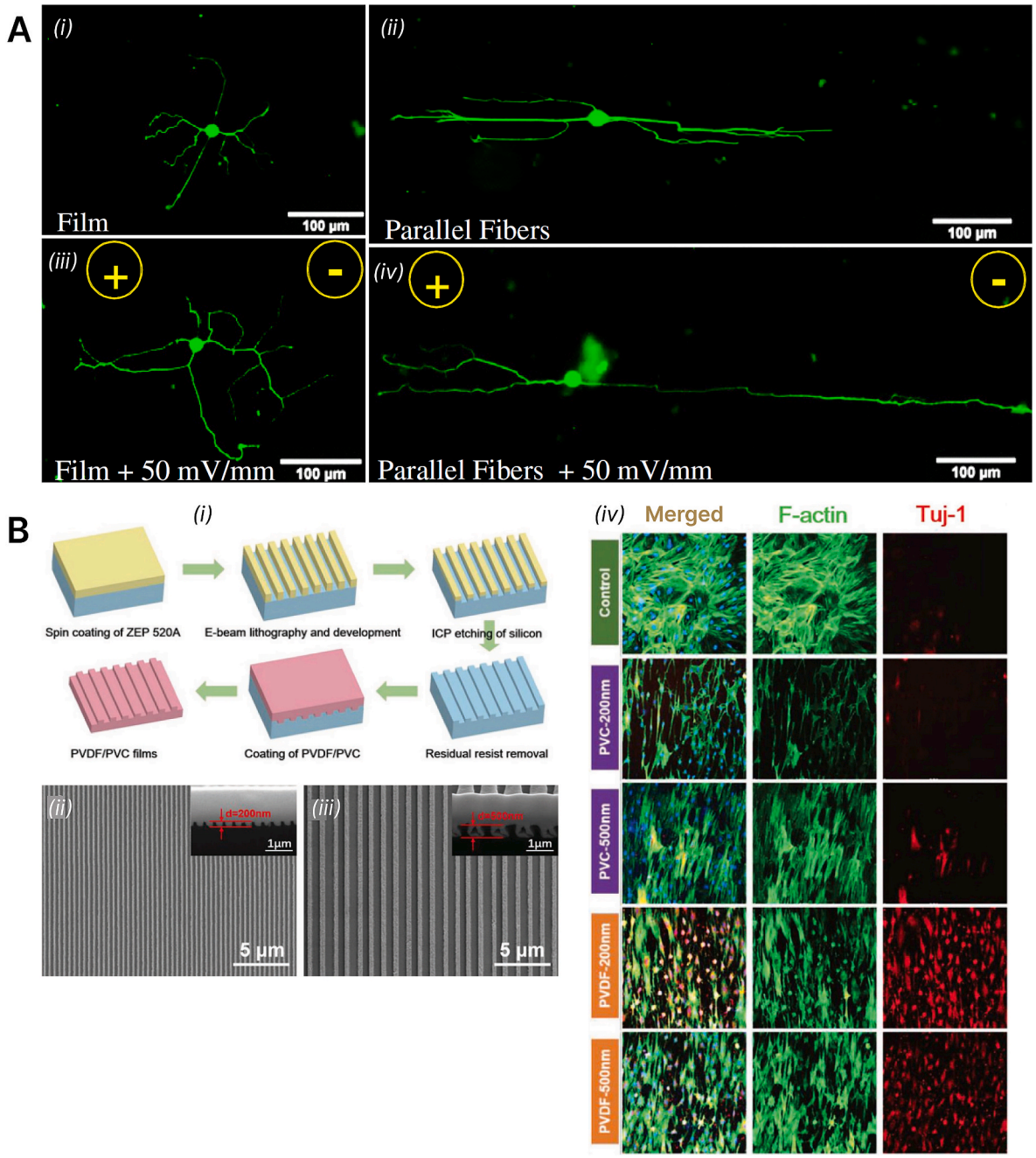

Fig. 18. Electrical stimulation and topographical cues from aligned fibers promote neurite outgrowth. (A) Immunofluorescent images of neurons on an unstimulated PLLA film *(i)*; on an unstimulated PLLA aligned fibrous scaffold *(ii)*; on an electrically stimulated (50 mV/mm; 8 h) PLLA film *(iii)*; and on a stimulated (50 mV/mm; 8 h) PLLA aligned scaffold. Green staining denotes β–III–tubulin–positive neurons. Reprinted from Ref. [94] with permission from IOP Science. (B) Piezoelectric PVDF nanostripe array structures. *(i)* The schematic of fabrication of PVDF films. SEM images of *(ii)* PVDF-200 (the ridge, groove, and height were all 200 nm) and *(iii)* PVDF-500 (the ridge, groove, and height were all 500 nm). *(iv)* Immunofluorescent staining of the neuron maker Tuj1 (red) after 7-day cultivation. Cell nuclei were stained with DAPI (blue), and F-actin with phalloidin-Alexa Fluor 488 (green). ICP: inductively coupled plasma. Reprinted from Ref. [67] with permission from Wiley.

means of collector rotating speed of 50, 100, 2000, or 3000 rpm (Fig. 17A). Nonaligned PVDF (50 rpm) was found to be the most appropriate for sustaining NSCs' survival and proliferation. Furthermore, nonaligned PVDF at 50 rpm favored both NSC maintenance and glial differentiation, whereas slightly aligned PVDF at 1000 rpm was the most appropriate for neuronal differentiation. SEM images of cells grown on the microfibrous scaffolds (Fig. 17A) indicated that the direction of neuronal cells' elongation was parallel to the direction of fiber alignment for moderately and highly aligned fibers (2000 and 3000 rpm, respectively), whereas the elongation directions were random for weakly aligned and nonaligned fibers (1000 and 50 rpm, respectively).

Lee and Arinzeh [49] have evaluated differentiation of human neural stem/progenitor cells (hNSCs/NPCs) on P(VDF-TrFE) nano- and microfibrous scaffolds with either random or aligned structure. hNSCs/NPCs differentiated mostly into β-III tubulin–positive cells and had the greatest average neurite length on micron-sized annealed aligned scaffolds [49]. Neurites of the DRG extend radially on randomly oriented P(VDF-TrFE) scaffolds (Fig. 17B–D), whereas aligned fibrous mats direct neurite outgrowth at all fiber dimensions (Fig. 17C–E) [65]. Moreover, extended neurite length of primary rat neurons on aligned PLLA/Fe_3O_4

fibers has been demonstrated (Fig. 17F–H) [129]. Some authors [45] have reported improved proliferation of rat neuronal-like cells (B65 cell line) on electrospun aligned PHB/chitosan scaffolds compared to randomly aligned ones. Similar results have been obtained with adipose-tissue–derived stem cells grown on aligned PHBV nanofibers [56].

In an *in vivo* study [101], aligned nanofibrous conduits of P(VDF-TrFE) promoted extension of $D\beta H^+$ axons and $GFAP^+$ processes farther than randomly aligned conduits did (Fig. 17I–L). That article showed SC viability *in vitro*, survival of transplanted SCs, and regeneration of axons within the conduits *in vivo* [101].

Coupling of aligned topographical cues with electric stimuli can have a synergistic enhancing effect on a variety of cellular activities, from cell adhesion to differentiation. Koppes et al. [94] have examined neurite outgrowth on either cast PLLA films or electrospun microfibers in the presence or absence of electrical stimulation (Fig. 18A). The results indicated that neurite extension rose by 74 % on the aligned fibers compared to control films (Fig. 18A, *i* vs. *iii*). Stimulation alone increased outgrowth by 32 % on films relative to unstimulated film controls (Fig. 18A, *i* vs. *ii*). The combination of topographical and biophysical cues resulted in a synergistic 126 % increase in the outgrowth relative to unstimulated film controls (Fig. 18A, *i* vs. *iv*). Thus, the topographical cues provided by the fibers were more dominant in supporting the extent and directionality of the neurite outgrowth as compared to the electrical stimulation alone.

Zhang et al. [67] have fabricated piezoelectric PVDF nanostripe array structures powered by cell adhesion and migration to investigate the synergistic effect of piezoelectricity and nanotopography on the proliferation, focal-adhesion formation, and neuron-like differentiation of rBMSCs (Fig. 18B). PVDF films with distinct stripe arrays and identically structured polyvinyl chloride (PVC) films were replicated from homostructural silicon molds (Fig. 18B, *i–ii*). Compared with that on TCP, vinculin expression (measured by fluorescent staining reflecting cell adhesion) was significantly higher on both PVDF and PVC nanoscale stripe arrays. Meanwhile, no statistically significant differences in vinculin expression were detected between the PVDF and PVC groups. Therefore, topography rather than piezoelectricity plays a crucial part in cell adhesion and proliferation. Concerning the differentiation of rBMSCs, significantly more cells positive for Tuj1 (a neuron marker) were found on the PVDF interfaces in comparison with TCP and PVC (Fig. 18B, *iii*). This result suggested that piezoelectricity rather than nanotopography of a stripe array nanostructure can enhance neuron-like differentiation of rBMSCs.

Magnetoresponsive materials offer various benefits not only for activation of piezoelectric materials in a magnetic field but also for creation of aligned micro- and nanostructures for nerve scaffolds [104,159]. Zhang et al. [104] have prepared magnetoelectric nanochains based on magnetostrictive Fe_3O_4 and piezoelectric $BaTiO_3$ (Fe_3O_4@$BaTiO_3$), which were subsequently incorporated into a biomimetic hydrogel and oriented by means of an external magnetic field, allowing for orientation of the hydrogel microfibers along the nanochains. The combination of the topological and electrical cues in this scaffold synergistically enhanced the expression of neural functional proteins and facilitated synapse remodeling and neural regeneration. Other materials combining piezoelectric stimulation with aligned topography cues are reported elsewhere [29,30,46–49,65,66,70,101].

7. Conclusions, challenges, and prospects

Numerous strategies to enhance nerve regeneration have been introduced, based either on piezoelectric stimulation alone or on a combination with additional topographical, biochemical, and biophysical factors. Piezoelectric biomaterials have several advantages, such as biocompatible electrical signal output matching the physiology and mechanical strength of soft tissues. Piezoelectric conduits can repair a neural tissue in a way similar to the natural processes occurring inside the ECM. Furthermore, piezoelectric stimulation does not require

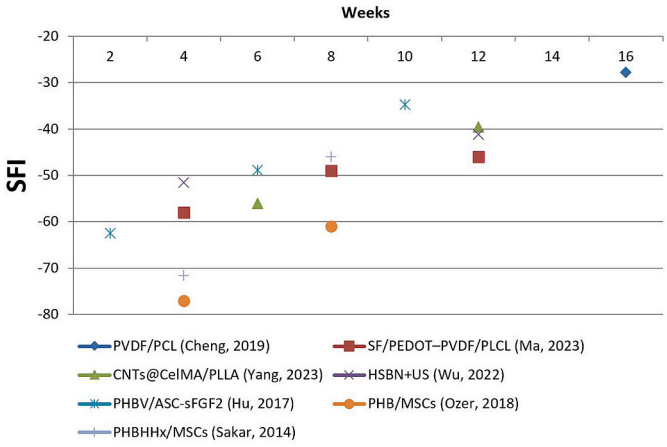

Fig. 19. A comparison of SFI values achieved through the use of piezoelectric NGCs.

auxiliary devices, such as electrodes and wires. Magnetoelectric scaffolds made of a piezoelectric matrix doped with magnetic particles as well as alternative magnetoelectric materials and composites are even more promising than ultrasound-driven piezoelectric scaffolds, despite still being mostly untested in nerve-regenerative applications. Magnetic fields are harmless to cells and tissues in a wide range of parameters and can also penetrate deeply into the human body without attenuation and tissue heating. Accordingly, a noninvasive wireless efficient approach to neural tissue engineering may get into clinical practice.

In addition to piezoelectric functionality, the advantage of aligned fiber morphology for neural regeneration has been proven in many studies [44–47,49,65–67,70,94,101]; hence, the greatest scientific potential lies in a combination of an aligned topography with piezoelectric stimulation. Besides, the effects of aligned topologies should be compared with those of piezoelectricity to determine the predominant factor for robust nerve regeneration.

Current achievements in the field of nerve regeneration induced by piezoelectric biomaterials *in vivo*, judging by the SFI, are compared in Fig. 19. In the papers presented, the periods of observation are limited to only 12 weeks or less, with only one study [31] where the regeneration process was evaluated during 16 weeks. Therefore, more prolonged *in vivo* assays would be worthwhile in which the SFI would be close to zero, corresponding to complete nerve restoration.

Table 6 lists some available FDA-approved commercial NGCs. Most of them are tubular hollow constructs with nonporous nonfibrous structures based on PCL, PGA, or collagen. Among these, only NeuraGen 3D has an aligned fibrous topography. Although these conduits have been proved to be biocompatible and biodegradable, the lack of bioactivity results in rather poor regenerative capacity. On the contrary, piezoelectric NGCs with an aligned topography produce impressive biological outcomes, as discussed in this review. Nonetheless, their potential has so far not been implemented in clinical practice for the following possible reasons. First, the techniques for preparation of piezoelectric conduits (e.g., electrospinning) with tailored properties are still at the laboratory stage. Furthermore, there is no standardization of mass production of piezoelectric materials and conduits for neural tissue engineering because a number of critical questions remain mostly unaddressed. A number of studies on piezoelectric scaffolds and conduits for nerve repair are focused on exploring materials' physicochemical properties such as morphology, chemical composition, and mechanical properties. On the other hand, data on their piezoelectric functionality are seldom reported. Key information about piezoelectric stimuli is still lacking including the optimal value for inducing maturity of neurons as well as long-term safety of electrical stimulation delivery though piezoelectric platforms. Moreover, the exact piezoelectric mechanisms governing cell behavior are not fully understood, thus necessitating

Table 6
Commercial FDA-approved NGCs.

Conduit and manufacturer	Year of approval	Composition	Biological model in clinical trial	Outcomes
NeuraGen 3D by Integra LifeSciences	2014	Core-shell tube with type I collagen shell and core made of collagen-glycosaminoglycan	Rat sciatic nerve gap of 10 mm	Significant improvement over hollow conduits; axon regeneration comparable to that of autograft
Neurolac by Polyganics Inc.	2003	PCL hollow tube	Digital nerve gap of up to 5 mm and 10-mm sciatic nerve gap	Sufficient recovery, albeit not statistically significantly different from the control; issues with swelling and degradation rate
NeuraGen by Integra LifeSciences	2001	Hollow tube based on type I collagen	Digital nerve 12.5-mm gap and median nerve 20-mm gap	4 of 12 patients: excellent sensibility; 5 of 12: good; 2 of 12: no recovery. Neuroma formation cases
NeuroMatrix and NeuroFlex by Collagen Matrix Inc.	2001	Hollow tube based on type I collagen	–	No publications available on testing. Recommended for up to 25-mm gaps.
Neurotube by Synovis	1999	PGA hollow tube	Digital nerve <4-mm gap and median nerve 30-mm gap	Good recovery of motor and sensory functions, albeit not significantly different from the control

additional investigation. From a biomaterial perspective, it is also not known how well the piezoelectric behavior is maintained long-term during contact with these cells. In fact, only a few studies have addressed piezoelectric measurements in culture media [160]. We believe that more insight into piezoelectric quantitative assays is crucial for addressing these issues and thus should allow for precise control over piezoelectric stimulation. We propose that piezoelectric characteristics should be quantified by piezoelectric force microscopy (PFM), which will lead to a better understanding of the mechanisms associated with cell–material interactions at the nanoscale. Future studies can also focus on measuring the piezoelectric activity *in situ* to elucidate how piezoelectricity contributes to axon regeneration. These issues highlight the need to standardize piezoelectric measurement setups to facilitate comparisons of results obtained by different research groups. Finally, it would be of interest to couple these piezoelectric setups with artificial intelligence interfaces for constant monitoring of such piezoelectric stimulation and to assess the response of neural cells overtime. Although challenges still exist, this review can give some important clues and inspiration to researchers for further progress in the development of novel piezoelectric biomaterials for neural tissue engineering.

CRediT authorship contribution statement

Lada E. Shlapakova: Conceptualization, Funding acquisition, Methodology, Writing – original draft. **Maria A. Surmeneva:** Conceptualization, Supervision, Writing – original draft. **Andrei L. Kholkin:** Conceptualization, Project administration, Supervision, Writing – review & editing. **Roman A. Surmenev:** Conceptualization, Funding acquisition, Methodology, Supervision, Writing – original draft, Writing – review & editing.

Declaration of competing interest

The authors declare that they have no known competing financial interests or personal relationships that could have appeared to influence the work reported in the paper “Revealing an important role of piezoelectric polymers in nervous-tissue regeneration: a Review” submitted to Materials Today Bio.

Data availability

No data was used for the research described in the article.

Acknowledgements

The research was carried out at National Research Tomsk Polytechnic University. The support from the Ministry of Science and Higher Education (grant agreement # 075-15-2021-588 of June 1, 2021) and from the Russian Science Foundation [#22-13-20043 (the part dealing with piezoelectric-effect of PLLA)] is acknowledged. A part of this work was developed within the scope of the project CICECO-Aveiro Institute of Materials, UIDB/50011/2020 and UIDP/50011/2020, financed by national funds through the FCT/MEC and, when appropriate, co-financed by FEDER under the PT2020 Partnership Agreement. The English language was corrected and certified by shevchuk-editing.com.

References

[1] S. Lee, M. Patel, R. Patel, Electrospun nanofiber nerve guidance conduits for peripheral nerve regeneration: a review, Eur. Polym. J. 181 (2022) 111663.
[2] P. Zarrintaj, et al., Conductive biomaterials as nerve conduits: recent advances and future challenges, Appl. Mater. Today 20 (2020) 100784.
[3] S. Behtaj, J.A.K. Ekberg, J.A. St John, Advances in electrospun nerve guidance conduits for engineering neural regeneration, Pharmaceutics 14 (2) (2022).
[4] S. Houshyar, A. Bhattacharyya, R. Shanks, Peripheral nerve conduit: materials and structures, ACS Chem. Neurosci. 10 (8) (2019) 3349–3365.
[5] Hinüber, C., et al., Hierarchically Structured Nerve Guidance Channels Based on Poly-3-Hydroxybutyrate Enhance Oriented Axonal Outgrowth. (1878-7568 (Electronic))..
[6] V.O. Castro, C. Merlini, Aligned electrospun nerve conduits with electrical activity as a strategy for peripheral nerve regeneration, Artif. Organs 45 (8) (2021) 813–818.
[7] P. Duffy, et al., Synthetic bioresorbable poly-α-hydroxyesters as peripheral nerve guidance conduits; a review of material properties, design strategies and their efficacy to date, Biomater. Sci. 7 (12) (2019) 4912–4943.
[8] T. Aydin, et al., Graphene based materials in neural tissue regeneration, in: K. Turksen (Ed.), Cell Biology and Translational Medicine, Volume 3: Stem Cells, Bio-Materials and Tissue Engineering, Springer International Publishing, Cham, 2018, pp. 129–142.
[9] P. Fattahi, et al., A review of organic and inorganic biomaterials for neural interfaces, Adv. Mater. 26 (12) (2014) 1846–1885.
[10] C. Ribeiro, et al., Piezoelectric polymers as biomaterials for tissue engineering applications, Colloids Surf. B Biointerfaces 136 (2015) 46–55.
[11] Y. Ma, et al., Piezoelectric conduit combined with multi-channel conductive scaffold for peripheral nerve regeneration, Chem. Eng. J. 452 (2023) 139424.
[12] H. Javidi, et al., Preparation and characterization of self-stimuli conductive nerve regeneration conduit using co-electrospun nanofibers filled with gelatin-chitosan hydrogels containing polyaniline-graphene-ZnO nanoparticles, International Journal of Polymeric Materials and Polymeric Biomaterials (2022) 1–11.
[13] S. Das, et al., In vivo studies of silk based gold nano-composite conduits for functional peripheral nerve regeneration, Biomaterials 62 (2015) 66–75.
[14] D. Yucel, G.T. Kose, V. Hasirci, Polyester based nerve guidance conduit design, Biomaterials 31 (7) (2010) 1596–1603.
[15] Yu, W., et al., A Novel Electrospun Nerve Conduit Enhanced by Carbon Nanotubes for Peripheral Nerve Regeneration. (1361-6528 (Electronic))..
[16] H. Ozer, et al., Regenerative potential of chitosan-coated poly-3-hydroxybutyrate conduits seeded with mesenchymal stem cells in a rat sciatic nerve injury model, Int. J. Neurosci. 128 (9) (2018) 828–834.
[17] W. Hu, et al., Enhancing proliferation and migration of fibroblast cells by electric stimulation based on triboelectric nanogenerator, Nano Energy 57 (2019) 600–607.
[18] W. Jing, et al., Study of electrical stimulation with different electric-field intensities in the regulation of the differentiation of PC12 cells, ACS Chem. Neurosci. 10 (1) (2018) 348–357.
[19] A.N. Koppes, et al., Electrical stimulation of schwann cells promotes sustained increases in neurite outgrowth, Tissue Eng. 20 (3–4) (2013) 494–506.

[20] A.N. Koppes, A.M. Seggio, D.M. Thompson, Neurite outgrowth is significantly increased by the simultaneous presentation of Schwann cells and moderate exogenous electric fields, J. Neural. Eng. 8 (4) (2011) 046023.
[21] W. Jing, et al., Constructing conductive conduit with conductive fibrous infilling for peripheral nerve regeneration, Chem. Eng. J. 345 (2018) 566–577.
[22] B. Guo, et al., Electroactive porous tubular scaffolds with degradability and non-cytotoxicity for neural tissue regeneration, Acta Biomater. 8 (1) (2012) 144–153.
[23] Y. Qian, et al., 3D manufacture of gold nanocomposite channels facilitates neural differentiation and regeneration, Adv. Funct. Mater. 28 (14) (2018) 1707077.
[24] Z.-F. Zhou, et al., Electrospinning of PELA/PPY fibrous conduits: promoting peripheral nerve regeneration in rats by self-originated electrical stimulation, ACS Biomater. Sci. Eng. 2 (9) (2016) 1572–1581.
[25] C. Phamornnak, et al., Instructive electroactive electrospun silk fibroin-based biomaterials for peripheral nerve tissue engineering, Biomater. Adv. 141 (2022) 213094.
[26] A.-P. Yu, et al., Comparative effects of implanted electrodes with differing contact patterns on peripheral nerve regeneration and functional recovery, Neurosci. Res. 145 (2019) 22–29.
[27] A. Marino, et al., Piezoelectric nanotransducers: the future of neural stimulation, Nano Today 14 (2017) 9–12.
[28] P. Chen, et al., Ultrasound-driven electrical stimulation of peripheral nerves based on implantable piezoelectric thin film nanogenerators, Nano Energy 86 (2021) 106123.
[29] Y. Yang, et al., Engineering a wirelessly self-powered and electroconductive scaffold to promote peripheral nerve regeneration, Nano Energy 107 (2023) 108145.
[30] Y. Tai, et al., Modulation of piezoelectric properties in electrospun PLLA nanofibers for application-specific self-powered stem cell culture platforms, Nano Energy 89 (2021) 106444.
[31] Y. Cheng, et al., 3D structured self-powered PVDF/PCL scaffolds for peripheral nerve regeneration, Nano Energy 69 (2020) 104411.
[32] W. Guo, et al., Self-powered electrical stimulation for enhancing neural differentiation of mesenchymal stem cells on graphene–poly (3, 4-ethylenedioxythiophene) hybrid microfibers, ACS Nano 10 (5) (2016) 5086–5095.
[33] L. Wu, et al., Recent advances in the preparation of PVDF-based piezoelectric materials 11 (1) (2022) 1386–1407.
[34] F. Barbosa, F.C. Ferreira, J.C. Silva, Piezoelectric electrospun fibrous scaffolds for bone, articular cartilage and osteochondral tissue engineering, Int. J. Mol. Sci. 23 (6) (2022) 2907.
[35] D. Khare, B. Basu, A.K. Dubey, Electrical stimulation and piezoelectric biomaterials for bone tissue engineering applications, Biomaterials 258 (2020) 120280.
[36] M.T. Chorsi, et al., Piezoelectric biomaterials for sensors and actuators, Adv. Mater. 31 (1) (2019) 1802084.
[37] Y. Qian, et al., Mechano-informed biomimetic polymer scaffolds by incorporating self-powered zinc oxide nanogenerators enhance motor recovery and neural function, Small 16 (32) (2020) 2000796.
[38] Y. Qian, et al., Boron nitride nanosheets functionalized channel scaffold favors microenvironment rebalance cocktail therapy for piezocatalytic neuronal repair, Nano Energy 83 (2021) 105779.
[39] A.H. Rajabi, M. Jaffe, T.L. Arinzeh, Piezoelectric materials for tissue regeneration: a review, Acta Biomater. 24 (2015) 12–23.
[40] J. Tao, et al., A review: polyacrylonitrile as high-performance piezoelectric materials, Nano Energy 118 (2023) 108987.
[41] A. Zaszczynska, P. Sajkiewicz, A. Gradys, Piezoelectric Scaffolds as smart Materials for neural tissue engineering, Polymers 12 (2020), https://doi.org/10.3390/polym12010161.
[42] S. Askari, Z.A. Bozcheloei, Piezoelectric composites in neural tissue engineering: material and fabrication techniques, Journal of Composites and Compounds 4 (10) (2022) 37–46.
[43] D. Xu, et al., Piezoelectric biomaterials for neural tissue engineering, Smart Medicine 2 (2) (2023) e20230002.
[44] E. Masaeli, et al., Fabrication, characterization and cellular compatibility of poly (hydroxy alkanoate) composite nanofibrous scaffolds for nerve tissue engineering, PLoS One 8 (2) (2013) e57157.
[45] A. Karimi Tar, et al., Biodegradation and cellular evaluation of aligned and random poly (3-hydroxybutyrate)/chitosan electrospun scaffold for nerve tissue engineering applications, Mater. Technol. 35 (2) (2020) 92–101.
[46] J.A. Orkwis, et al., Development of a piezoelectric PVDF-TrFE fibrous scaffold to guide cell adhesion, proliferation, and alignment, Macromol. Biosci. 20 (9) (2020) 2000197.
[47] J.A. Orkwis, et al., Mechanical stimulation of a bioactive, functionalized PVDF-TrFE scaffold provides electrical signaling for nerve repair applications, Biomater. Adv. 140 (2022) 213081.
[48] S. Wu, et al., Aligned fibrous PVDF-TrFE scaffolds with Schwann cells support neurite extension and myelination in vitro, J. Neural. Eng. 15 (5) (2018) 056010.
[49] Y.-S. Lee, T.L. Arinzeh, The influence of piezoelectric scaffolds on neural differentiation of human neural stem/progenitor cells, Tissue Eng. 18 (19–20) (2012) 2063–2072.
[50] O. Suwantong, et al., In vitro biocompatibility of electrospun poly (3-hydroxybutyrate) and poly (3-hydroxybutyrate-co-3-hydroxyvalerate) fiber mats, Int. J. Biol. Macromol. 40 (3) (2007) 217–223.
[51] Karimi, A., et al., Poly(hydroxybutyrate)/chitosan Aligned Electrospun Scaffold as a Novel Substrate for Nerve Tissue Engineering. (2277-9175 (Print))..
[52] L.R. Lizarraga-Valderrama, et al., Unidirectional neuronal cell growth and differentiation on aligned polyhydroxyalkanoate blend microfibres with varying diameters, Journal of Tissue Engineering and Regenerative Medicine 13 (9) (2019) 1581–1594.
[53] Y.-Z. Bian, et al., Evaluation of poly (3-hydroxybutyrate-co-3-hydroxyhexanoate) conduits for peripheral nerve regeneration, Biomaterials 30 (2) (2009) 217–225.
[54] H. Xie, et al., Enhanced proliferation and differentiation of neural stem cells grown on PHA films coated with recombinant fusion proteins, Acta Biomater. 9 (8) (2013) 7845–7854.
[55] M.P. Prabhakaran, E. Vatankhah, S. Ramakrishna, Electrospun aligned PHBV/collagen nanofibers as substrates for nerve tissue engineering, Biotechnol. Bioeng. 110 (10) (2013) 2775–2784.
[56] F. Hu, et al., Neuronally differentiated adipose-derived stem cells and aligned PHBV nanofiber nerve scaffolds promote sciatic nerve regeneration, Biochem. Biophys. Res. Commun. 489 (2) (2017) 171–178.
[57] E. Masaeli, et al., Peptide functionalized polyhydroxyalkanoate nanofibrous scaffolds enhance Schwann cells activity, Nanomed. Nanotechnol. Biol. Med. 10 (7) (2014) 1559–1569.
[58] T.M. Dinis, et al., 3D multi-channel bi-functionalized silk electrospun conduits for peripheral nerve regeneration, J. Mech. Behav. Biomed. Mater. 41 (2015) 43–55.
[59] A. Singh, et al., Mechanical properties of spinal nerve roots subjected to tension at different strain rates, J. Biomech. 39 (9) (2006) 1669–1676.
[60] G. Liu, et al., Stress and strain analysis on the anastomosis site sutured with either epineurial or perineurial sutures after simulation of sciatic nerve injury, Neural regeneration research 7 (29) (2012) 2299.
[61] J. Kerns, et al., Mechanical properties of the human tibial and peroneal nerves following stretch with histological correlations, Anat. Rec. 302 (11) (2019) 2030–2039.
[62] B.L. Rydevik, et al., An in vitro mechanical and histological study of acute stretching on rabbit tibial nerve, J. Orthop. Res. 8 (5) (1990) 694–701.
[63] Y. Li, et al., Developments of advanced electrospinning techniques: a critical review, Advanced Materials Technologies 6 (11) (2021) 2100410.
[64] F. Qi, et al., A conductive network enhances nerve cell response, Addit. Manuf. 52 (2022) 102694.
[65] Y.-S. Lee, G. Collins, T. Livingston Arinzeh, Neurite extension of primary neurons on electrospun piezoelectric scaffolds, Acta Biomater. 7 (11) (2011) 3877–3886.
[66] Z. Liu, et al., Cell-traction-triggered on-demand electrical stimulation for neuron-like differentiation, Adv. Mater. 33 (51) (2021) 2106317.
[67] X. Zhang, et al., Piezoelectric nanotopography induced neuron-like differentiation of stem cells, Adv. Funct. Mater. 29 (22) (2019) 1900372.
[68] G.G. Genchi, et al., P (VDF-TrFE)/BaTiO3 nanoparticle composite films mediate piezoelectric stimulation and promote differentiation of SH-SY5Y neuroblastoma cells, Adv. Healthcare Mater. 5 (14) (2016) 1808–1820.
[69] E.G. Fine, et al., Improved nerve regeneration through piezoelectric vinylidenefluoride-trifluoroethylene copolymer guidance channels, Biomaterials 12 (8) (1991) 775–780.
[70] L.C. Lins, et al., Effect of polyvinylidene fluoride electrospun fiber orientation on neural stem cell differentiation, J. Biomed. Mater. Res. B Appl. Biomater. 105 (8) (2017) 2376–2393.
[71] Z. He, et al., Electrospun PVDF nanofibers for piezoelectric applications: a review of the influence of electrospinning parameters on the β phase and crystallinity enhancement, Polymers 13 (2021), https://doi.org/10.3390/polym13020174.
[72] G. Kalimuldina, et al., A review of piezoelectric PVDF film by electrospinning and its applications, Sensors 20 (2020), https://doi.org/10.3390/s20185214.
[73] O. Ero-Phillips, M. Jenkins, A. Stamboulis, Tailoring crystallinity of electrospun plla fibres by control of electrospinning parameters, Polymers 4 (3) (2012).
[74] A.S. Pryadko, et al., Comprehensive study on the reinforcement of electrospun PHB scaffolds with composite magnetic Fe3O4–rGO fillers: structure, physico-mechanical properties, and piezoelectric response, ACS Omega 7 (45) (2022) 41392–41411.
[75] R.S. Kurusu, N.R. Demarquette, Surface modification to control the water wettability of electrospun mats, Int. Mater. Rev. 64 (5) (2019) 249–287.
[76] Y. Ding, et al., Electrospun polyhydroxybutyrate/poly(ε-caprolactone)/58S sol–gel bioactive glass hybrid scaffolds with highly improved osteogenic potential for bone tissue engineering, ACS Appl. Mater. Interfaces 8 (27) (2016) 17098–17108.
[77] J. Si, et al., Biomimetic composite scaffolds based on mineralization of hydroxyapatite on electrospun poly(ε-caprolactone)/nanocellulose fibers, Carbohydr. Polym. 143 (2016) 270–278.
[78] W. Jang, et al., PVdF/graphene oxide hybrid membranes via electrospinning for water treatment applications, RSC Adv. 5 (58) (2015) 46711–46717.
[79] J. Wang, et al., Influence of surface roughness on contact angle hysteresis and spreading work, Colloid Polym. Sci. 298 (8) (2020) 1107–1112.
[80] S. Veeramasuneni, et al., Hydrophobicity of ion-plated PTFE coatings, Prog. Org. Coating 31 (3) (1997) 265–270.
[81] T. Onda, et al., Super-water-repellent fractal surfaces, Langmuir 12 (9) (1996) 2125–2127.
[82] T.T. Chau, et al., A review of factors that affect contact angle and implications for flotation practice, Adv. Colloid Interface Sci. 150 (2) (2009) 106–115.
[83] R.E. Johnson Jr., R.H. Dettre, Contact angle hysteresis, in: Contact Angle, Wettability, and Adhesion, American Chemical Society, 1964, pp. 112–135.
[84] M. Miwa, et al., Effects of the surface roughness on sliding angles of water droplets on superhydrophobic surfaces, Langmuir 16 (13) (2000) 5754–5760.
[85] N. Encinas, et al., Control of wettability of polymers by surface roughness modification, J. Adhes. Sci. Technol. 24 (11–12) (2010) 1869–1883.
[86] K.J. Kubiak, et al., Wettability versus roughness of engineering surfaces, Wear 271 (3) (2011) 523–528.

[87] L. Chen, C. Yan, Z. Zheng, Functional polymer surfaces for controlling cell behaviors, Mater. Today 21 (1) (2018) 38–59.
[88] G. Xia, et al., Piezoelectric charge induced hydrophilic poly(L-lactic acid) nanofiber for electro-topographical stimulation enabling stem cell differentiation and expansion, Nano Energy 102 (2022) 107690.
[89] S. Heidari-Keshel, et al., Surface modification of Poly Hydroxybutyrate (PHB) nanofibrous mat by collagen protein and its cellular study, Mater. Technol. 31 (13) (2016) 799–805.
[90] X. Lu, et al., Stemness maintenance and massproduction of neural stem cells on poly L-lactic acid nanofibrous membrane based on piezoelectriceffect, Small 18 (13) (2022) 2107236.
[91] F. Pires, et al., Neural stem cell differentiation by electrical stimulation using a cross-linked PEDOT substrate: expanding the use of biocompatible conjugated conductive polymers for neural tissue engineering, Biochim. Biophys. Acta Gen. Subj. 1850 (6) (2015) 1158–1168.
[92] Y. Zhang, et al., Magnetoelectric nanoparticles incorporated biomimetic matrix for wireless electrical stimulation and nerve regeneration, Adv. Healthcare Mater. 10 (16) (2021) 2100695.
[93] S. Kim, et al., Electrically conductive polydopamine–polypyrrole as high performance biomaterials for cell stimulation in vitro and electrical signal recording in vivo, ACS Appl. Mater. Interfaces 10 (39) (2018) 33032–33042.
[94] A.N. Koppes, et al., Neurite outgrowth on electrospun PLLA fibers is enhanced by exogenous electrical stimulation, J. Neural. Eng. 11 (4) (2014) 046002.
[95] J. Jacob, et al., Piezoelectric smart biomaterials for bone and cartilage tissue engineering, Inflamm. Regen. 38 (1) (2018) 2.
[96] T. Marques-Almeida, et al., Electroactive materials surface charge impacts neuron viability and maturation in 2D cultures, ACS Appl. Mater. Interfaces 15 (26) (2023) 31206–31213.
[97] M. Mohseni, et al., Preparation and characterization of self-electrical stimuli conductive gellan based nano scaffold for nerve regeneration containing chopped short spun nanofibers of PVDF/MCM41 and polyaniline/graphene nanoparticles: physical, mechanical and morphological studies, Int. J. Biol. Macromol. 167 (2021) 881–893.
[98] X.-Z. Chen, et al., Magnetically driven piezoelectric soft microswimmers for neuron-like cell delivery and neuronal differentiation, Mater. Horiz. 6 (7) (2019) 1512–1516.
[99] R. Zhang, et al., Ultrasonic-driven electrical signal-iron ion synergistic stimulation based on piezotronics induced neural differentiation of mesenchymal stem cells on FeOOH/PVDF nanofibrous hybrid membrane, Nano Energy 87 (2021) 106192.
[100] P. Aebischer, et al., Piezoelectric guidance channels enhance regeneration in the mouse sciatic nerve after axotomy, Brain Res. 436 (1) (1987) 165–168.
[101] Y.-S. Lee, et al., Enhanced noradrenergic axon regeneration into schwann cell-filled PVDF-TrFE conduits after complete spinal cord transection, Biotechnol. Bioeng. 114 (2) (2017) 444–456.
[102] H.-F. Guo, et al., Piezoelectric PU/PVDF electrospun scaffolds for wound healing applications, Colloids Surf. B Biointerfaces 96 (2012) 29–36.
[103] M. Hoop, et al., Ultrasound-mediated piezoelectric differentiation of neuron-like PC12 cells on PVDF membranes, Sci. Rep. 7 (1) (2017) 1–8.
[104] Zhang, Y., et al., Magneto Manipulation from the Growth of Fe 3 O 4@ BaTiO 3 Nanochain to Extra Cellular Topographical and Electrical Cues Regulation. Available at: SSRN 4407516..
[105] C. Shuai, et al., A strawberry-like Ag-decorated barium titanate enhances piezoelectric and antibacterial activities of polymer scaffold, Nano Energy 74 (2020) 104825.
[106] F. Qi, et al., Magnetic-driven wireless electrical stimulation in a scaffold, Compos. B Eng. 237 (2022) 109864.
[107] T. Gordon, A.W. English, Strategies to promote peripheral nerve regeneration: electrical stimulation and/or exercise, Eur. J. Neurosci. 43 (3) (2016) 336–350.
[108] E. Doron-Mandel, M. Fainzilber, M. Terenzio, Growth control mechanisms in neuronal regeneration, FEBS Lett. 589 (14) (2015) 1669–1677.
[109] Q. Liu, B. Song, Electric field regulated signaling pathways, Int. J. Biochem. Cell Biol. 55 (2014) 264–268.
[110] W. Xue, et al., Anisotropic scaffolds for peripheral nerve and spinal cord regeneration, Bioact. Mater. 6 (11) (2021) 4141–4160.
[111] T. Fukazawa, et al., Electrical stimulation accelerates neuromuscular junction formation through ADAM19/neuregulin/ErbB signaling in vitro, Neurosci. Lett. 545 (2013) 29–34.
[112] J.C. Weaver, R.D. Astumian, The response of living cells to very weak electric fields: the thermal noise limit, Science 247 (4941) (1990) 459–462.
[113] M. Manthorpe, et al., Laminin promotes neuritic regeneration from cultured peripheral and central neurons, J. Cell Biol. 97 (6) (1983) 1882–1890.
[114] D.J. Goldberg, D.W. Burmeister, Looking into growth cones, Trends Neurosci. 12 (12) (1989) 503–506.
[115] R. Balint, N.J. Cassidy, S.H. Cartmell, Conductive polymers: towards a smart biomaterial for tissue engineering, Acta Biomater. 10 (6) (2014) 2341–2353.
[116] Q. Li, Q. Wang, Ferroelectric polymers and their energy-related applications, Macromol. Chem. Phys. 217 (11) (2016) 1228–1244.
[117] C. Wan, C.R. Bowen, Multiscale-structuring of polyvinylidene fluoride for energy harvesting: the impact of molecular-, micro-and macro-structure, J. Mater. Chem. A 5 (7) (2017) 3091–3128.
[118] P. Martins, A.C. Lopes, S. Lanceros-Mendez, Electroactive phases of poly (vinylidene fluoride): determination, processing and applications, Prog. Polym. Sci. 39 (4) (2014) 683–706.
[119] B. Tandon, J.J. Blaker, S.H. Cartmell, Piezoelectric materials as stimulatory biomedical materials and scaffolds for bone repair, Acta Biomater. 73 (2018) 1–20.
[120] N. Weber, et al., Characterization and in vitro cytocompatibility of piezoelectric electrospun scaffolds, Acta Biomater. 6 (9) (2010) 3550–3556.
[121] T.L. Arinzeh, N. Weber, M. Jaffe, Electrospun Electroactive Polymers for Regenerative Medicine Applications, Google Patents, 2018.
[122] R.F. Valentini, et al., Electrically charged polymeric substrates enhance nerve fibre outgrowth in vitro, Biomaterials 13 (3) (1992) 183–190.
[123] L.N. Novikova, et al., Biodegradable poly-β-hydroxybutyrate scaffold seeded with Schwann cells to promote spinal cord repair, Biomaterials 29 (9) (2008) 1198–1206.
[124] Y.-J. Ren, et al., Enhanced differentiation of human neural crest stem cells towards the Schwann cell lineage by aligned electrospun fiber matrix, Acta Biomater. 9 (8) (2013) 7727–7736.
[125] H. Zhang, et al., Electrospun piezoelectric scaffold with external mechanical stimulation for promoting regeneration of peripheral nerve injury, Biomacromolecules 24 (7) (2023) 3268–3282.
[126] P. Wu, et al., Ultrasound-driven in vivo electrical stimulation based on biodegradable piezoelectric nanogenerators for enhancing and monitoring the nerve tissue repair, Nano Energy 102 (2022) 107707.
[127] M. Patel, et al., Iron ion-releasing polypeptide thermogel for neuronal differentiation of mesenchymal stem cells, Biomacromolecules 21 (1) (2019) 143–151.
[128] A.V. Singh, et al., Investigation of in vitro cytotoxicity of the redox state of ionic iron in neuroblastoma cells, J. Neurosci. Rural Pract. 3 (3) (2012) 301–310.
[129] C.D.L. Johnson, et al., Injectable, magnetically orienting electrospun fiber conduits for neuron guidance, ACS Appl. Mater. Interfaces 11 (1) (2019) 356–372.
[130] H. Wang, J. Zhang, K. Tashiro, Phase transition mechanism of poly(l-lactic acid) among the α, δ, and β forms on the basis of the reinvestigated crystal structure of the β form, Macromolecules 50 (8) (2017) 3285–3300.
[131] A. Sultana, et al., Human skin interactive self-powered wearable piezoelectric bio-e-skin by electrospun poly-l-lactic acid nanofibers for non-invasive physiological signal monitoring, J. Mater. Chem. B 5 (35) (2017) 7352–7359.
[132] J. Wang, et al., In vitro and in vivo studies of electroactive reduced graphene oxide-modified nanofiber scaffolds for peripheral nerve regeneration, Acta Biomater. 84 (2019) 98–113.
[133] J.L. Funnell, et al., Assessing the combination of magnetic field stimulation, iron oxide nanoparticles, and aligned electrospun fibers for promoting neurite outgrowth from dorsal root ganglia in vitro, Acta Biomater. 131 (2021) 302–313.
[134] A.P. Boskhomdzhiev, et al., Biodegradation kinetics of poly(3-hydroxybutyrate)-based biopolymer systems, Biochemistry (Moscow) Supplement Series B: Biomedical Chemistry 4 (2) (2010) 177–183.
[135] X.-H. Qu, et al., In vivo studies of poly(3-hydroxybutyrate-co-3-hydroxyhexanoate) based polymers: biodegradation and tissue reactions, Biomaterials 27 (19) (2006) 3540–3548.
[136] A.S. Pryadko A, et al., Electrospun magnetic composite poly-3-hydroxybutyrate/magnetite scaffolds for biomedical applications: composition, structure, magnetic properties, and biological performance, ACS Appl. Bio Mater. 5 (8) (2022) 3999–4019.
[137] A. Pryadko, M.A. Surmeneva, R.A. Surmenev, Review of hybrid materials based on polyhydroxyalkanoates for tissue engineering applications, Polymers 13 (11) (2021).
[138] P.-N. Mohanna, G. Terenghi, M. Wiberg, Composite PHB-GGF conduit for long nerve gap repair: a long-term evaluation, Scand. J. Plast. ReConstr. Surg. Hand Surg. 39 (3) (2005) 129–137.
[139] A. Hazari, et al., A resorbable nerve conduit as an alternative to nerve autograft in nerve gap repair, Br. J. Plast. Surg. 52 (8) (1999) 653–657.
[140] A. Mosahebi, M. Wiberg, G. Terenghi, Addition of fibronectin to alginate matrix improves peripheral nerve regeneration in tissue-engineered conduits, Tissue Eng. 9 (2) (2003) 209–218.
[141] R.C. Young, G. Terenghi, M. Wiberg, Poly-3-hydroxybutyrate (PHB): a resorbable conduit for long-gap repair in peripheral nerves, Br. J. Plast. Surg. 55 (3) (2002) 235–240.
[142] P.N. Mohanna, et al., A composite poly-hydroxybutyrate–glial growth factor conduit for long nerve gap repairs, J. Anat. 203 (6) (2003) 553–565.
[143] S.J. Armstrong, et al., ECM molecules mediate both Schwann cell proliferation and activation to enhance neurite outgrowth, Tissue Eng. 13 (12) (2007) 2863–2870.
[144] Liu, Z., et al., A Magnetically Responsive Nanocomposite Scaffold Combined with Schwann Cells Promotes Sciatic Nerve Regeneration upon Exposure to Magnetic Field. (1178-2013 (Electronic))..
[145] D.F. Kalbermatten, et al., Schwann cell strip for peripheral nerve repair, J. Hand Surg. 33 (5) (2008) 587–594.
[146] M. Sakar, et al., The effect of poly (3-hydroxybutyrate-co-3-hydroxyhexanoate) (PHBHHx) and human mesenchymal stem cell (hMSC) on axonal regeneration in experimental sciatic nerve damage, Int. J. Neurosci. 124 (9) (2014) 685–696.
[147] A.M. Hart, M. Wiberg, G. Terenghi, Exogenous leukaemia inhibitory factor enhances nerve regeneration after late secondary repair using a bioartificial nerve conduit, Br. J. Plast. Surg. 56 (5) (2003) 444–450.
[148] Hu, F., et al., Neuronally Differentiated Adipose-Derived Stem Cells and Aligned PHBV Nanofiber Nerve Scaffolds Promote Sciatic Nerve Regeneration. (1090-2104 (Electronic))..
[149] S. Karimi, et al., Alginate-magnetic short nanofibers 3D composite hydrogel enhances the encapsulated human olfactory mucosa stem cells bioactivity for

potential nerve regeneration application, Int. J. Biol. Macromol. 167 (2021) 796–806.
[150] M.-H. Beigi, et al., In vivo integration of poly(ε-caprolactone)/gelatin nanofibrous nerve guide seeded with teeth derived stem cells for peripheral nerve regeneration, J. Biomed. Mater. Res. 102 (12) (2014) 4554–4567.
[151] X. Jiang, et al., Nanofibrous nerve conduit-enhanced peripheral nerve regeneration, Journal of Tissue Engineering and Regenerative Medicine 8 (5) (2014) 377–385.
[152] Z. Chen, et al., NSC-derived extracellular matrix-modified GelMA hydrogel fibrous scaffolds for spinal cord injury repair, NPG Asia Mater. 14 (1) (2022) 20.
[153] H.B. Wang, et al., Varying the diameter of aligned electrospun fibers alters neurite outgrowth and Schwann cell migration, Acta Biomater. 6 (8) (2010) 2970–2978.
[154] M.F.B. Daud, et al., An aligned 3D neuronal-glial co-culture model for peripheral nerve studies, Biomaterials 33 (25) (2012) 5901–5913.
[155] Amini, S. and M.K. White, Neuronal Cell Culture Methods and Protocols..
[156] Q. Quan, et al., Aligned fibers enhance nerve guide conduits when bridging peripheral nerve defects focused on early repair stage, Neural Regeneration Research 14 (5) (2019).
[157] L. Huang, et al., A compound scaffold with uniform longitudinally oriented guidance cues and a porous sheath promotes peripheral nerve regeneration in vivo, Acta Biomater. 68 (2018) 223–236.
[158] Hurtado, A., et al., Robust CNS Regeneration after Complete Spinal Cord Transection Using Aligned Poly-L-Lactic Acid Microfibers. (1878-5905 (Electronic))..
[159] L. Xia, et al., Controllable growth of spiral ganglion neurons by magnetic colloidal nanochains, Nano Today 44 (2022) 101507.
[160] L.T. Beringer, et al., An electrospun PVDF-TrFe fiber sensor platform for biological applications, Sensor Actuator Phys. 222 (2015) 293–300.